



**GEOMATICS CANADA
OPEN FILE 97e**

Ring of Fire: satellite monitoring of environmental indicators



**W. Chen, D. Janzen, M.T. Bonney, R.A. Fernandes, R.H. Fraser, L. He, J. Li,
F. Mohammadimanesh, N.H. Short, J.J. van der Sanden, Y. Zhang, B.-H. Choe,
N. Djamai, H. Drouin, G. Hong, S.G. Leblanc, S. Leipe, G. Richardson,
S.V. Samsonov, L. Sun, and S. Wang**

2025

**GEOMATICS CANADA
OPEN FILE 97e**

Ring of Fire: satellite monitoring of environmental indicators

W. Chen, D. Janzen, M.T. Bonney, R.A. Fernandes, R.H. Fraser, L. He, J. Li, F. Mohammadimanesh, N.H. Short, J.J. van der Sanden, Y. Zhang, B.-H. Choe, N. Djamai, H. Drouin, G. Hong, S.G. Leblanc, S. Leipe, G. Richardson, S.V. Samsonov, L. Sun, and S. Wang

2025

© His Majesty the King in Right of Canada, as represented by the Minister of Natural Resources, 2025

Information contained in this publication or product may be reproduced, in part or in whole, and by any means, for personal or public non-commercial purposes, without charge or further permission, unless otherwise specified.

You are asked to:

- exercise due diligence in ensuring the accuracy of the materials reproduced;
- indicate the complete title of the materials reproduced, and the name of the author organization; and
- indicate that the reproduction is a copy of an official work that is published by Natural Resources Canada (NRCan) and that the reproduction has not been produced in affiliation with, or with the endorsement of, NRCan.

Commercial reproduction and distribution is prohibited except with written permission from NRCan. For more information, contact NRCan at copyright-droitdauteur@nrcan-rncan.gc.ca.

This publication is available for free download through the NRCan Open Science and Technology Repository (<https://ostrnrcan-dostrnrcan.canada.ca/>).

Recommended citation

Chen, W., Janzen, D., Bonney, M.T., Fernandes, R.A., Fraser, R.H., He, L., Li, J., Mohammadimanesh, F., Short, N.H., van der Sanden, J.J., Zhang, Y., Choe, B.-H., Djamai, N., Drouin, H., Hong, G., Leblanc, S.G., Leipe, S., Richardson, G., Samsonov, S.V., Sun, L., and Wang, S., 2025. Ring of Fire: satellite monitoring of environmental indicators; Geomatics Canada, Open File 97e, 34 p. <https://doi.org/10.4095/pr9qyys1yt>

Publications in this series have not been edited; they are released as submitted by the author.

ISSN 2292-7875
ISBN 978-0-660-97621-1
Catalogue No. M103-3/97-2025E-PDF
<https://doi.org/10.4095/pr9qyys1yt>

Table of Contents

Executive summary	i
Indicator 1. Surface Water Dynamics	1
Indicator 2. Snow Cover Phenology	4
Indicator 3. Snow depth	7
Indicator 4. Lake Ice Extent	10
Indicator 5. Terrestrial Water Storage.....	13
Indicator 6. Caribou Lichen Availability	16
Indicator 7. Beaver Engineering.....	19
Indicator 8. Land Cover	22
Indicator 9. Vegetation Cover and Density	25
Indicator 10. Permafrost.....	28
Indicator 11. Terrain Deformation	31
Acknowledgement.....	34

Cover photo: A landscape photo of Northern Ontario. Photograph by R.H. Fraser

Executive summary

Canada requires evidence-based strategies to support sustainable development and long-term prosperity as part of its nation-building objectives. One such approach is the Critical Minerals Strategy, which aims to strengthen domestic resource security and economic resilience. The Ring of Fire (ROF) assessment area in northern Ontario has been identified as a region with significant potential for critical minerals development. To achieve a balance among economic growth, environmental stewardship, and social equity, rigorous impact assessments are essential.

The *Terms of Reference for the Regional Assessment in the Ring of Fire Area* delineate four primary assessment priorities: community well-being, cultural and spiritual well-being, social and economic equity, and environmental health. These priorities were established through extensive consultation processes and are informed by the perspectives and concerns expressed by Indigenous communities in the region.

The assessment priority for “healthy environment relationships” includes “water and river systems, including flows”; “wildlife and wildlife habitat, including species at risk, migratory birds, and fish and fish habitat”; “peatlands and other unique environments”; “forest ecosystems, including plants”; “climate change adaptation”; “biodiversity”; and “air quality”. Using satellite observations, the Canada Centre for Mapping and Earth Observation, along with its partners, has developed eleven environmental indicators that contribute to assessing healthy environment relationships. Specifically, we have created five indicators for “water and river systems”: *surface water*, *snow cover*, *snow depth*, *lake ice extent*, and *total water storage*. For “wildlife and wildlife habitat”, we contribute two indicators: *caribou lichen availability* and *beaver engineering*. Two indicators, *land cover* and *vegetation cover and density*, contribute to several assessment priorities, including “forest ecosystems,” “peatlands and other unique environments,” and “biodiversity.” Additionally, we have developed two indicators to support “climate change adaptation”: *permafrost* and *terrain deformation*.

For each of these eleven environmental indicators, we first establish their relevance to the assessment priorities they aim to support. This is followed by a brief description of the methodology for deriving the indicator using satellite observations and some preliminary results. Indigenous communities play a crucial role in this process, having helped to identify priorities and concerns, providing local knowledge and context, and collaborating on the collection and validation of ground-truth data.

As demonstrated in this report, satellite images can cover large areas repeatedly and are thus especially suitable for timely regional assessment. With long historical records dating back to the 1980s, increasing spectral and geospatial accuracies, and application-ready data, satellite Earth observation data are poised to play a significant role in regional assessments. Further incorporation of Indigenous knowledge can enhance the accuracy and impact of these satellite-derived indicators, making them more useful for local decision-making. The final results for the eleven environmental indicators will be detailed in subsequent publications. We will also make these companion data products available to the public.

It is the intention that this report, and the data described therein, will be used, in partnership with Indigenous communities and other stakeholders, to inform environmental assessments, guide decision-making, and support sustainable management of the region’s natural resources.

Indicator 1. Surface Water Dynamics

Relevance to the ROF assessment priorities

The Ring of Fire (ROF) assessment region is dominated by large freshwater ecosystems that contain thousands of lakes and streams. According to the HydroLAKE database [1], there are about 19,000 lakes larger than 0.1 km² within this region. The region also hosts several major rivers, including the Albany, Moose, Winisk, Ekwana, and Attawapiskat rivers. However, road developments and mining explorations in this region may lead to disturbances of the freshwater ecosystems, altering evapotranspiration, surface water-groundwater interactions, and the role of surface water in the overall regional water budget. These processes can lead to changes in lake distribution and water level, and in some cases, the formation and disappearance of entire lakes.

One of the key assessment priorities for healthy environmental relationships is “Water and river systems, including flows” as listed in the “Terms of Reference for the Regional Assessment in the Ring of Fire (ROF) area.” Effective conservation and management of surface water resources in this region are therefore critical. Accurate monitoring is essential to track changes and inform decision-making. Detailed knowledge of surface water dynamics provides the foundation for understanding the changes in water in this region. Advances in remote sensing technologies provide efficient tools to map and monitor surface water changes.

Among various optical and SAR satellite sensors, Landsat sensors provide the most important data source for detecting/monitoring surface water changes because of their relatively high spatial resolution (30m), extensive spatial coverage, and long period (over 40 years) data records. With open access to the Landsat data archive, a few global/continental surface water products have been produced [2, 3]. Among these, the Global Surface Water (GSW) dataset, produced by the Joint Research Centre (JRC) of the European Commission, has been widely recognized and adopted. However, there are significant quality issues in the product, particularly in Canada’s north. For example, our examination of the monthly water

product over the Canadian landmass showed significant misclassifications between land and water

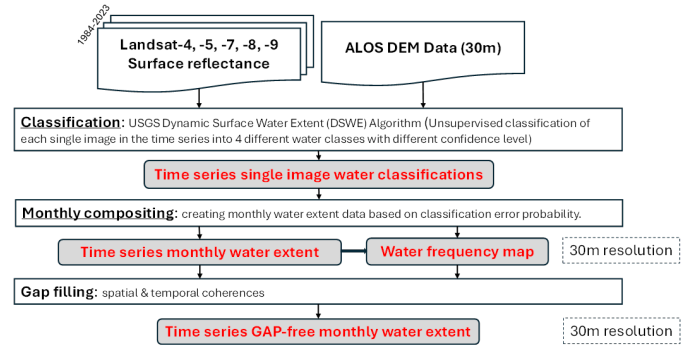


Fig. 1. The outline of the steps for generating surface water data using Landsat imagery.

for pixels affected by cloud and sensor anomalies [4]. Therefore, it is difficult to obtain actual surface water area from the GSW dataset and other available products for the ROF’s assessment applications, which require high temporal resolution and gap-free (e.g., monthly) datasets.

Methodology

To address the limitations of the current available surface water products, we developed a new approach, which is based on the Google Earth Engine (GEE) cloud computing platform, for generating high-quality, gap-free, monthly surface water products from the Landsat data. Figure 1 outlines the approach. The approach includes three key components: 1) Time series single-image water classifications: The Dynamic Surface Water Extent (DSWE), originally developed by USGS [5], was enhanced to classify each Landsat image in the time series into four different water classes with different confidence levels; 2) Monthly compositing: a novel algorithm based on classification error probabilities is used to create monthly water extent maps for the period of 1984 to 2023. Note that the monthly data will be used to generate a surface water frequency map over a region, where water frequency is defined as the percentage of a pixel that appears as water in the total available observations during a specific time period. This water frequency map will be used for gap filling of the monthly products; 3) Monthly gap filling: a newly developed spatial and temporal coherence algorithm is applied to fill gaps and

produce a time series of gap-free monthly surface water extent maps. These maps are also used to derive monthly surface water area statistics at various spatial scales (e.g. watersheds, ecoregions). For more detailed information about the approach, refer to Li et al. [6].

Indicator definition and early results

Figure 2(a) shows the monthly composited surface water extent over the ROF region. As shown, there are significant portions of areas showing no-data gaps due to cloud cover. Figure 2(b) shows the gap-filled surface water extent map by using our spatial and temporal coherence algorithm. Long time series (1984-2023) 30m resolution monthly surface water extent data over the ROF region was generated from our approach. This dataset provides baseline water data for the assessment analysis in the ROF region.

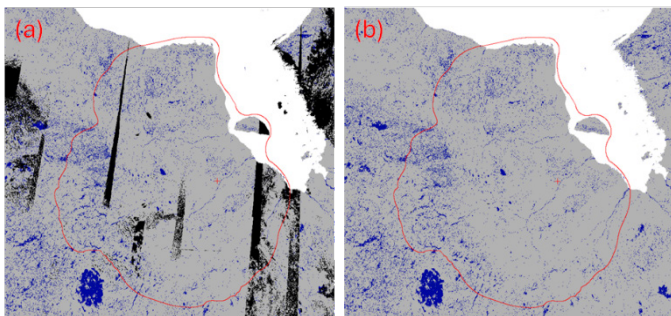


Fig. 2. The surface water extent map over the ROF assessment region for July 2000: (a) before gap-filling, (b) after gap-filling. The black color indicates the data gaps.

For the regional assessment of the ROF area regarding water, it is essential to address a key question: “Where is the water?” One indicator that helps answer the question is the surface water frequency (or probability) [7]. Figure 3 shows the surface water frequency from 1991 to 2020, providing information about overall surface water dynamics across the ROF area. On this map, pixels with values of 0% and 100% refer to permanent land and permanent water, respectively, during the 30-year period. Areas with a frequency ranging from 1% to 99% represent inundation areas, which appear as land and water at different times during the 30 years.

From the surface water frequency map, we calculated the permanent water area and inundation area in the ROF region, as well as the areas for lakes with different size categories following the

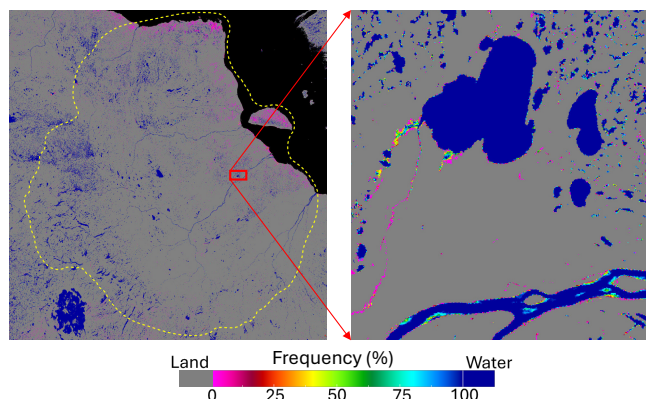


Fig. 3. The surface water frequency (probability) map over the ROF assessment region (yellow polygon) for the period of 1991 to 2020.

HydroLAKES database (Table 1). Note that these surface water area statistics can change with the time periods.

Table 1. Summary of lake area, inundation extent, and number of lakes with different size categories ($\geq 0.1 \text{ km}^2$ to $\geq 50 \text{ km}^2$) within the ROF assessment region.

Lake size	$\geq 0.1 \text{ km}^2$	$\geq 1 \text{ km}^2$	$\geq 5 \text{ km}^2$	$\geq 10 \text{ km}^2$	$\geq 50 \text{ km}^2$	All*
Lake numbers	18909	2056	287	118	19	
Permanent water (km ²)	11730	8161	4907	3810	1935	14700
Maximum Inundation* (km ²)	2368	894	432	330	153	8990
Medium Inundation* (km ²)	897	390	200	153	72	2470

*All means the surface water area for all the lakes and rivers in the ROF assessment region. Maximum inundation and medium inundation refer to inundation areas with frequencies $>0\%$ and $\geq 50\%$, respectively.

Conclusions and next steps

40-year (1984-2023) long-term gap-free monthly surface water extent datasets at 30m resolution over the ROF assessment region were generated from Landsat data using the approach developed at the Canada Centre for Mapping and Earth Observation. From the 30m monthly data, a surface water frequency map was derived, showing this region’s surface water dynamics over the period of 1991 to 2020.

For the next steps, we will examine the trends of surface water area changes in the ROF assessment region. The trends over the 40-year period will be analyzed at the sub-basin level, and a trend map will be generated. The monthly gap-free surface water extent data will be analyzed for specific sub-basins

to reveal local trends and seasonal patterns. The analysis and results are anticipated to be completed in 2026.

For more information, contact:

Junhua.Li@NRCan-RNCan.gc.ca,

Shusen.Wang@NRCan-RNCan.gc.ca.

References

- [1] Messenger, M.L., Lehner, B., Grill, G., Nedeva, I., and Schmitt, O., 2016. Estimating the volume and age of water stored in global lakes using a geo-statistical approach. *Natural Communications*, 7, 13603, doi:10.1038/ncomms13603.
- [2] Pekel, J.-F., Cottam, A., Gorelick, N., Belward, A.S., 2016. High-resolution mapping of global surface water and its long-term changes. *Nature* 540, 418-422.
- [3] Donchyts, G., Baart, F., Winsemius, H., Gorelick, N., Kwadijk, J., and van de Giesen, N., 2016. Earth's surface water change over the past 30 years. *Nature Clim Change* 6, 810–813 (2016). <https://doi.org/10.1038/nclimate3111>
- [4] Wang, Shusen, Junhua. Li, and Hazen A. J. Russell, 2023, Methods for Estimating Surface Water Storage Changes and Their Evaluations. *Journal of Hydrometeorology*, DOI: <https://doi.org/10.1175/JHM-D-22-0098.1>.
- [5] Jones, J.W., 2019. Improved automated detection of subpixel-scale inundation—Revised dynamic surface water extent (DSWE) partial surface water tests. *Remote Sensing* 11, 374.
- [6] Li, J., Wang, S., and Sun, L., 2025, Landsat-derived long-term monthly surface water datasets over Canada’s landmass. Geomatics Canada, Open File XXXX, 1.zip file. Doi:10.4095/xxxx
- [7] Natural Resources Canada. 2023. *Canada’s surface water frequency*. <https://open.canada.ca/data/en/dataset/2b76d117-d940-4ebb-bf26-91f768081c5f>

Indicator 2. Snow Cover Phenology

Relevance to the ROF assessment priorities

Snow is an Essential Climate Variable that reflects most solar radiation, which helps mitigate climate warming, and insulates the ground from winter air temperatures in cold regions like northern portions of the Ring of Fire Assessment Area, impacting permafrost distribution [1]. Snow cover phenology (e.g., the start and end dates of seasonal snow cover) is important for plants, including influencing when different species grow in the spring, and animals, including influencing migration patterns and timing. Snow is also important for society, including providing freshwater for drinking and farming. In the Assessment Area, winter roads are critical infrastructure for most Mushkegowuk and Matawa First Nation communities and resource extraction operations (Figure 1). Snow and ice phenology dictate how long these vital connections are viable each winter. Snow and ice loss in the spring can also trigger flooding along rivers, such as the 1986 flood, which forced the relocation of the Weenusk First Nation. On the other hand, spring snow loss opens up other transportation infrastructure (e.g., roads, runways) for easier travel.

The *Terms of Reference for the Regional Assessment in the Ring of Fire Area* recognize the importance of many of these aspects in their assessment priorities. The “*To be well together (Community wellbeing)*” priority includes infrastructure and economic development as components, and snow phenology (e.g., winter roads) is an important part of these. This is also the case for the *Social and Economic Equity* priority, especially components related to providing economic benefits and access to the land. Snow phenology is also critical for *Healthy Environment Relationships*, including components related to water, wildlife, plants, and climate change.

We developed this indicator for monitoring snow at a higher spatial detail (30m pixel size) than any other snow product available across Canada (e.g., 250+ m pixel size [2]). It was not feasible to investigate landscape-scale snow phenology across Canada before the creation of this product.

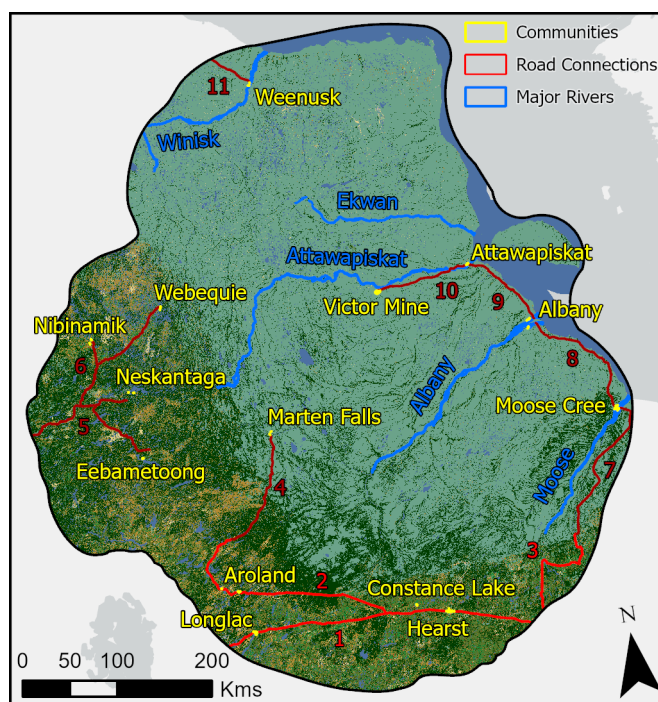


Fig. 1. Assessment Area, with locations of interest shown. Landcover classes match Indicator 8. Road groups are numbered, with permanent roads in lighter red and winter roads in darker red.

Methodology

Our methodology relies on two satellite constellations: Europe’s Sentinel-2 program and the United States’ Landsat program. Combined, these constellations collect images over almost the entire global land surface (and coastal oceans) and have done so approximately every 2-3 days since 2018 [3]. We gather all images collected over Canada and identify the status of each 30m pixel observation on the image collection date: snow (and ice), non-snow (i.e., land, water), unclear (i.e., clouds, shadows).

We built an algorithm [4] to calculate snow cover indicators for each pixel during each winter:

- **Start:** Start date of the first (or biggest) snow period
- **End:** End date of the last (or biggest) snow period
- **Length:** Number of days with snow cover in total (or in the biggest snow period)
- **Periods:** Number of snow periods (i.e., separated times with multiple confirmed snow observations)
- **Status:** Classification (e.g., continuous, snow free)

We do not obtain a clear observation every day because of satellite orbit frequencies and clouds. This means that timing-based indicators (i.e., start, end,

length) are identified by the middle date between two clear observations, with uncertainty quantified as half the length of the gap (i.e., \pm days).

Our algorithm has been tested in a variety of regions across North America and accounts for rare snow phenology patterns. We calculate indicators for each winter since 2018-2019 and can also provide multi-year averages. Validation assessments have shown that the snow end date performs well in all tests, and later snow melting generally corresponds to areas with thicker snow accumulation. Therefore, we use snow end dates to model and map snow depth (Indicator 2). Snow end generally has lower uncertainty than snow start (and length) since snow melt usually occurs in less cloudy conditions than snowfall.

For this report, we processed 30m snow cover phenology across the Assessment Area using the latest version of our methodology. We focus on snow end dates with less than 15 days of uncertainty in relation to land cover and locations of interest across the Assessment Area (Figure 1). Locations of interest include the developed areas of 14 communities (inc. Victor Mine), 11 road connections (Trans-Canada Highway, two permanent winter road feeders, and eight winter roads), and the primary channels of five major rivers where widths exceed 100m.

Results

Snow end dates vary generally by latitude across the Assessment Area, with earlier (e.g., mid-April) melting in the south and later (e.g., late May) melting in the north (Figure 2). Land cover does not strongly influence snow melt regionally in this mostly flat landscape, except for water vs. land (Figure 3). Ice on larger lakes and coastal Hudson Bay, especially, can persist well into June. On the other hand, water currents can cause early melt, with sea ice near the outflow of the Attawapiskat River south of Akimiski Island usually melting in March. Snow end dates can differ drastically due to yearly climate variability in southern portions of the Assessment Area, with warmer springs (e.g., 2021, 2024) triggering snow disappearance nearly a month earlier than colder springs (e.g., 2020).

The local variability in snow disappearance timing is a unique capability provided by this indicator. For example, in many tundra landscapes in the northern portion of the Assessment Area, local terrain influences snow end dates. In Figure 2A, we can see snow end dates differ by almost a month between more sheltered areas, which collect snow (e.g., the south-east shore of lakes), and nearby exposed areas where snow is blown away. Figure 2B shows Attawapiskat, where the airport and community infrastructure are cleared of snow earlier than the surrounding wetlands, which in turn are generally snow free before ice has melted on the Attawapiskat River.

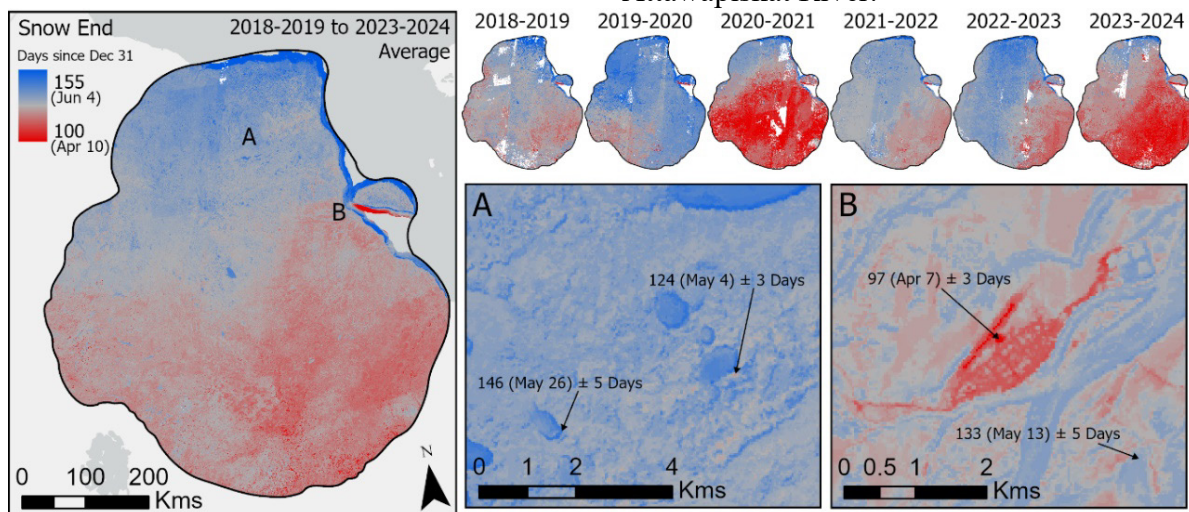


Fig. 2. Snow end date mapped across the Assessment Area. Left: Average across the six observed winters. Top right: Mapped for each winter. Bottom right: Local views of average snow end date for a tundra wetland (A; 84.24°W, 54.23°N) and Attawapiskat (B; 82.43°W, 52.92°N), with example dates \pm uncertainties shown. Results not provided for ocean 10+ km from the coast and where there was greater than 15 days uncertainty.

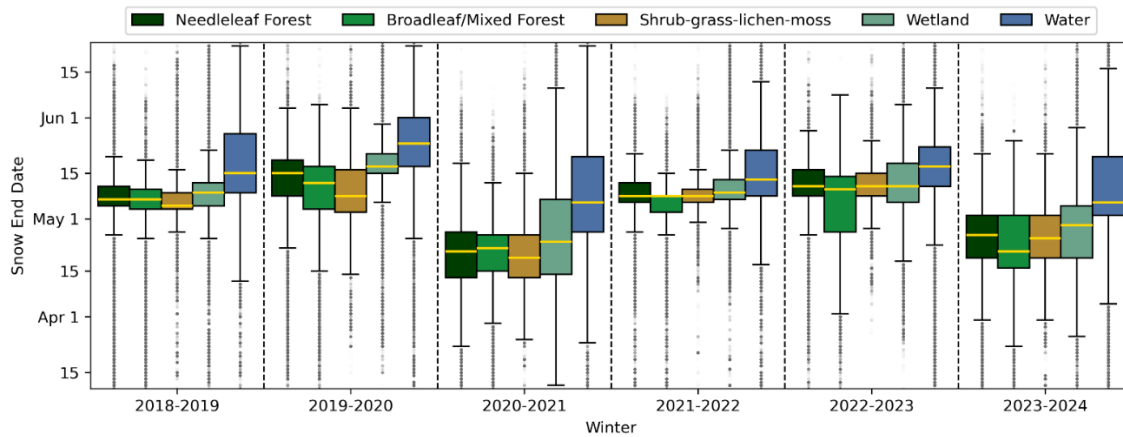


Fig. 3. Boxplots of snow end dates by land cover type for each mapped winter across the Assessment Area. See Indicator 8 for more details on land cover. Some classes are combined for simpler visualization.

We can monitor snow end dynamics in locations of interest, including communities like Attawapiskat, road connections and major rivers (Figure 4). Most follow a similar trajectory as the entire region, except for locations in the Weenusk First Nation that are less impacted by southern spring climate variability. Communities are generally clear of snow first, while winter roads maintain snow longer, and river ice longer still. Additional assessment shows that infrastructure-clearing efforts are observed, with communities free of snow a week earlier than their immediate natural (non-water) surroundings on average (earliest clearing average: 12 days earlier in Attawapiskat; latest: two days earlier in Moose Cree communities). Isolating airport runways would show even earlier relative clearing. These satellite-based timings can also provide valuable information on the yearly viability of winter roads and when rivers have been most at-risk of ice melt-induced flooding.

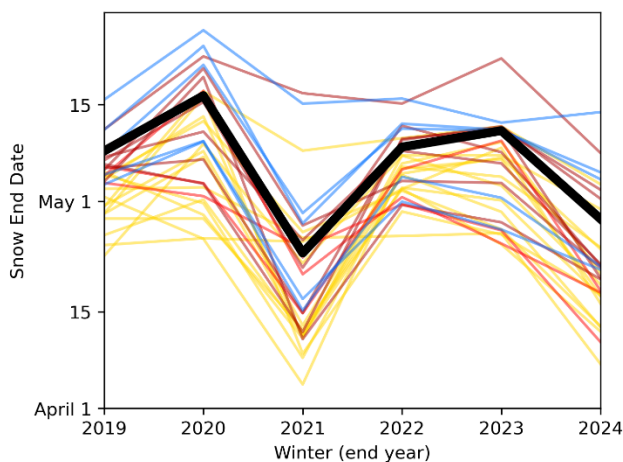


Fig. 4. Yearly median snow end dates for locations of interest. Colors match Figure 1. The black line represents the entire Assessment Area.

Conclusions and next steps

Yearly snow phenology map at 30 m resolution provides valuable insights for regions of interest like the Ring of Fire Assessment Area. Here, we demonstrate how the snow end date can be used to investigate landscape-scale snow loss variability in natural and developed settings. Snow end date is an indicator of peak snow depth, which impacts permafrost stability, seasonal cycles for plants and animals, community wellbeing, and other factors. Our snow depth and permafrost mapping work (Indicators 2 and 10) rely on these snow end dates. Development continues and is focused on reducing uncertainty in lower observation frequency areas, raising performance in some settings (e.g., forest), and national-scale validation. For more information: mitchellthurston.bonney@nrcan-rncan.gc.ca.

References

- [1] Global Climate Observing System, 2024. Essential Climate Variables. [Link](#).
- [2] Trishchenko, A.P., Ungureanu, C., 2024. Cumulative changes in minimum snow/ice extent over Canada and northern USA for 2000-2023. *Can. J. Remote Sens.* 50(1), 2371359.
- [3] Ju, J., Zhou, Q., Freitag, B., Roy, D.P., Zhang, H.K., Sridhar, M., ... Neigh, C.S.R., 2025. The Harmonized Landsat and Sentinel-2 version 2.0 surface reflectance dataset. *Remote Sens. Environ.* 324, 114723.
- [4] Bonney, M.T., Zhang, Y., 2025. Wide-area 30-m resolution snow dynamics from Harmonized Landsat Sentinel-2. *Under review at ISPRS J. Photogramm. Remote Sens.*

Indicator 3. Snow depth

Relevance to the ROF assessment priorities

The Ring of Fire (ROF) area is covered by snow for about six months a year. Snow has significant impacts on the environment and the way of life of First Nation communities, including the water conditions of lakes and rivers, water supply and spring flooding, winter roads and winter hunting/trapping activities, ground thawing/freezing and permafrost, soil moisture and terrestrial ecosystems, migration and habitats of animals. More importantly, snow conditions differ from place to place and from year to year, and they are changing with the long-term trend of global warming.

Snow depth is recorded at most climate stations, but the stations are sparsely distributed and are not representative of natural land conditions. Spatial distributions of snow depth have been mapped using very coarse spatial detail, with resolutions ranging from 1 km to 20 km. Such coarse maps are not practically useful for communities and regional impact assessments. Figure 1 shows snow maps at different levels of detail. Intensive fieldwork and using drones or airplanes can map snow depth at high spatial resolutions (small pixel sizes). However, they can only cover limited time and areas, and the cost is high.

We developed a new method to model and map snow depth with 30m pixel size and quantify their changes with climate.

Methodology

The method is based on the Northern Ecosystem Soil Temperature (NEST) model, which considers the detailed processes of snow dynamics, including snow accumulation after snowfall, snow compaction, sublimation, melt, and changes in snow temperature, density and depth [2]. The model uses a parameter (F_{snow}) to represent variations in snow input due to snow redistribution by wind and potential biases in the precipitation data. The F_{snow} for each grid cell is estimated based on snow cover end date (S_{end}), which is mapped from satellite data (see Indicator 2). Our analysis and other studies show that F_{snow} is relatively stable from one year to the next for a given site [1].

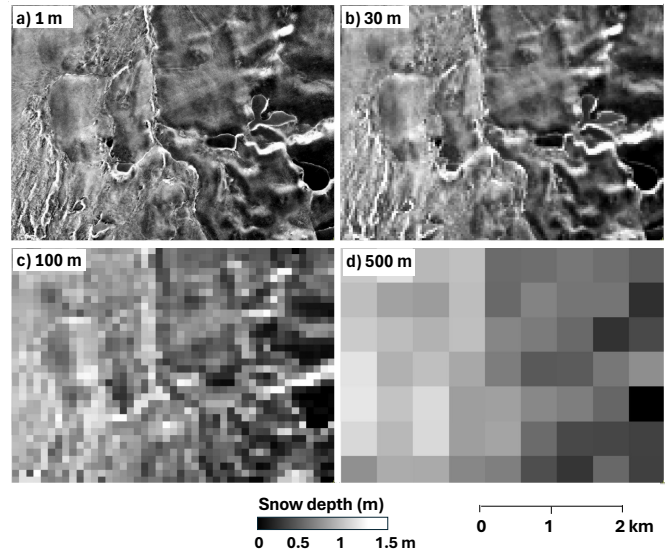


Fig. 1. Snow depth maps for the same area with different spatial resolutions. Panel 'a' shows the snow depth with 1m resolution measured on April 16, 2012, in an area in northern Alaska [1]. The other panels were re-sampled using averages from panel 'a' to different resolutions.

Therefore, we can use the average F_{snow} calculated from 2018 to 2024 to run the model in other years when S_{end} data are not available. To model and map snow efficiently at a 30m pixel size, we ran the model for various possible F_{snow} values, vegetation and ground conditions for a small number of sites and then linearly interpolated the model results to each 30m pixel based on its location and local conditions, including its S_{end} mapped from satellites.

We mapped snow depth across the Hudson Bay Lowlands (HBL) from 1950 to 2100. The climate data from 1950 to 2024 are from ERA5-Land [3]. The future climate from 2025 to 2100 is based on a projection of a Canadian Regional Climate Model under a medium-low greenhouse gas emission scenario using representative concentration pathways (RCP) 4.5 [4]. The land cover types and peat thickness maps specifically for the HBL regions are from Ian Olthof and Emily Ogden, respectively, of Environment and Climate Change Canada (personal communications). Leaf area index was calculated from satellite data (Indicator 9).

Early results

Figure 2 shows an example of the mapped mean snow depth in March 2018. Snow depth varied significantly at landscape scales mainly due to snow redistribution by wind. Snow depth also varies from coast to inland and from north to south due to climate gradients. Our spatially detailed snow depth map shows the locations of roads, winter roads and railroads (right panel in Fig. 2) although we did not consider complex processes of human impacts.

Figure 3 shows April mean snow depths in the recent decade (2014-2025), and in the 2090s under a medium climate warming scenario (RCP 4.5). Snow in April will be shallower with climate warming.

Figure 4a shows changes in annual mean air temperature from 1950 to 2100 in Attawapiskat (52.926 °N, 82.429 °W; see Fig. 1 left panel). Figures 4b and 4c show the modelled mean snow depth in May and annual snow cover days from 1950 to 2100 in a typical shrub peatland without redistribution of snow by wind ($F_{snow} = 1$). It shows that the duration of winter road viability will be shorter with climate warming.

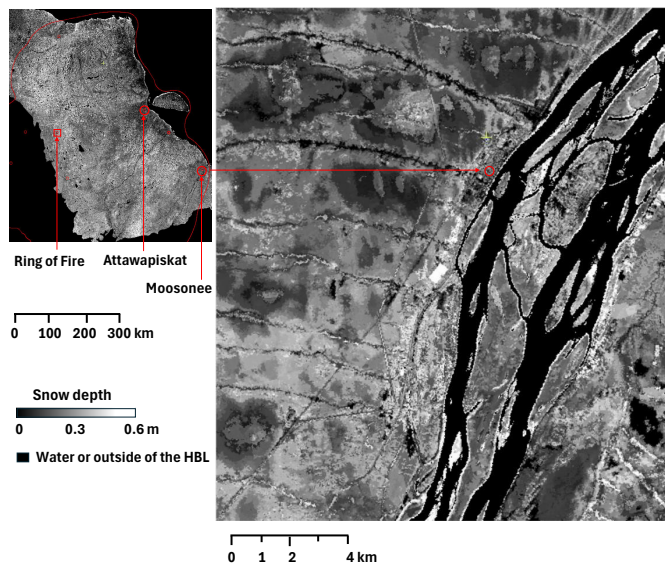


Fig. 2. Mapped mean snow depth in March 2018. The left panel shows a large part of the ROF impact assessment area in the HBL (its boundary is shown in the red curve), and the right panel is a small area around the town of Moosonee shown in a red circle.

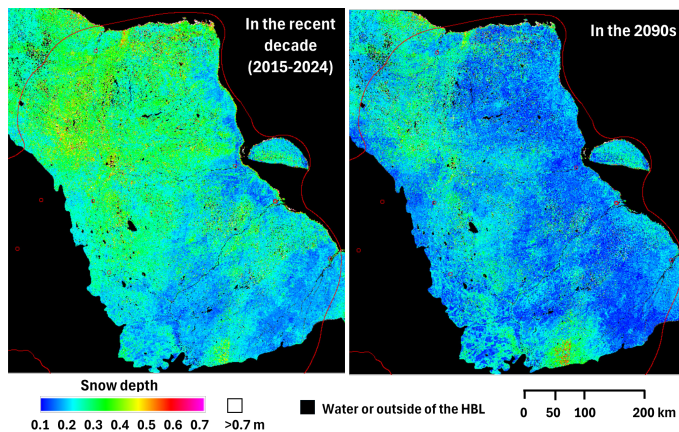


Fig. 3. Mapped April mean snow depth in the last decade (2014-2025) and in the 2090s under a medium-low climate warming scenario (RCP 4.5) for a large part of the ROF impact assessment area in the HBL (its boundary is shown in the red curve).

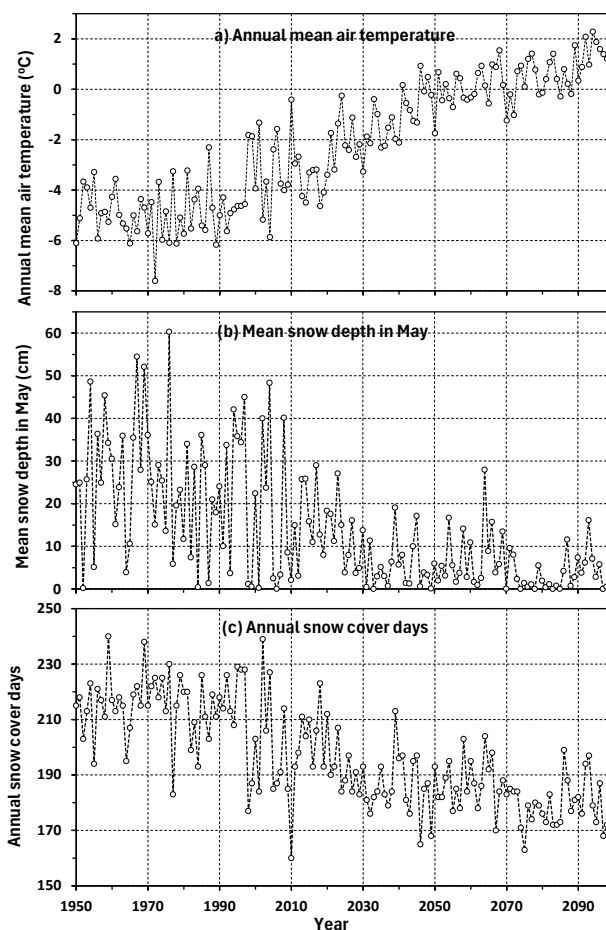


Fig. 4. Annual mean air temperature and modelled mean snow depth in May and annual snow cover days at a shrub peatland area near Attawapiskat (52.926 °N, 82.429 °W). The climate data from 2025 to 2100 are based on the projection under a medium-low climate warming scenario (RCP4.5).

Conclusions and next steps

Snow, as an essential climate variable, not only affects the climate system at broad-scales, it also has significant impacts on the local and regional environment and the life of local peoples. Previous maps of snow depth are too coarse for First Nation communities. We developed a new method to model and map snow depth with a 30m pixel size. The results show large variations at landscape scales and with climate gradients, and changes climate warming. This information is important for hunting/trapping activities, land-use and infrastructure development, and adaptation to the changing climate.

We tested this method based on observations in two areas in northern Alaska. We will continue to validate results across the HBL. We will extend snow depth products to cover the entire ROF assessment area based on the needs of the local communities and impact assessment requirements. We will also consider other potential climate change projections. The results will be published later, and the data will be released on the Open Science and Data Platform. For more information, contact yu.zhang @NRCan-RNCan.gc.ca.

Acknowledgements

This study is funded by Park Canada Agency under the Hudson Bay-James Bay Biodiversity Conservation and Carbon Sequestration Initiative. Glen Brown of Ontario Ministry of Natural Resources provided climate data at several stations. Emily Ogden, Ian Olthof, and Taylor Biccum in Environment and Climate Change Canada provided a land cover map, a peat thickness map, and a sub-pixel water fraction map over the HBL. Xiping Wang processed station climate data and assessed gridded climate data. And Gang Hong generated a leaf area index map.

References

- [1] Parr, C., M. Sturm, and C. Larsen (2020). Snowdrift landscape patterns: An arctic investigation. *Water Resources Research*, 56. doi: 10.1029/2020wr027823.
- [2] Zhang, Y., W. Chen, and J. Cihlar (2003). A process-based model for quantifying the impact

- of climate change on permafrost thermal regimes. *Journal of Geophysical Research*, 108, D22, 4695. doi: 10.1029/2002JD003354
- [3] Muñoz-Sabater, J. E. Dutra, A. Agustí-Panareda, et al. (2021). ERA5-Land: a state-of-the-art global reanalysis dataset for land applications. *Earth System Scientific Data*, 13, 4349-4383. doi: 10.5194/essd-13-4349-2021
- [4] Scinocca, J. F. V. V. Kharin, Y. Jiao, et al. (2016). Coordinated global and regional climate modeling. *Journal of Climate*, 29, 17-35. doi: 10.1175/JCLI-D-15-0161.1

Indicator 4. Lake Ice Extent

Relevance to the ROF assessment priorities

Lake ice represents an important component of the winter landscape in most regions of Canada, including in the Ring of Fire assessment area. The interactions between lake ice and the environment are significant and pertain to e.g. climatic, hydrological, biological, social, cultural, and economic conditions [1]. According to the *Terms of Reference for the Regional Assessment in the Ring of Fire Area* these conditions represent overarching assessment priorities. As an example, lake ice provides an effective base for roads and trails that facilitate seasonal access to isolated sites such as remote communities and traditional hunting / fishing grounds. In this capacity, lake ice contributes to more specific assessment priorities such as community wellbeing, cultural wellbeing, and economic equity. Through its interactions with water, wildlife, biodiversity and climate, lake ice is also of relevance to the “Healthy Environment Relationships” assessment priority.

Here we will focus on a lake ice measure known as lake ice extent. This measure characterizes the total surface area of a lake that is covered by ice—as a function of time. As such, it is an indicator of changes in lake ice phenology, i.e. in the seasonal timing of ice freeze-up and breakup and in the duration of the ice-on season. Potential causes of variation in these indicators are either natural or man-made and include changes such as in climate, weather, water levels, and water temperature.

Methodology

Thanks to the capacity to consistently acquire geolocated data over large areas, Earth Observation (EO) satellites make excellent tools to collect up-to-date lake ice extent information. Relative to optical EO satellites, Synthetic Aperture Radar (SAR) satellites represent a more reliable, practical, and cost-effective tool to characterize lake ice extent. This is due to their unique capacity to acquire good quality, high-resolution images under adverse weather and low daylight conditions. Such conditions are frequently encountered in Canada and

have contributed to decisions by the Government of Canada to invest in SAR satellite systems such as the RADARSAT Constellation Mission (RCM) [2]. Conventional methods to determine lake ice extent from SAR images involve visual interpretation. Increasing data volumes, expanding information requirements, and budget constraints make these methods unsustainable. As such, we are developing automated methods to characterize lake ice extent by means of SAR satellite images [3,4]. At this time, our objective is to develop methods specifically for the extraction of lake ice extent information from RCM Compact Polarimetry (CP) image products. The pronounced sensitivity of radar sensors to variability in lake ice wetness, which is a function of air temperature, calls for the development of two different approaches to map the evolving extent of lake ice during the freeze-up and breakup seasons. Original models to classify ice and water lie at the core of each approach and are bookended by radar image pre- and post-processing steps. The classification models are being developed by means of a machine learning algorithm and RCM image data for three sites that collectively extend from southern to northern Canada. As such, these sites represent a wide range of lake ice conditions. The lakes comprised in the Ring of Fire assessment area provide a good opportunity to test the performance of our classification models.

Indicator definition and early results

In brief, *lake ice extent*, our primary indicator, equals the total surface area of a lake that is covered by ice rather than water. Lake ice extent information can be presented in various ways, i.e. in the form of maps or numbers. Numerically, lake ice extent is commonly expressed as a percentage of the total surface area of the lake. This percentage is typically referred to as *lake ice concentration*. Our methods are designed to produce both output forms. Comparison of lake ice extent information for different dates allows for the derivation of secondary indicators such as the dates

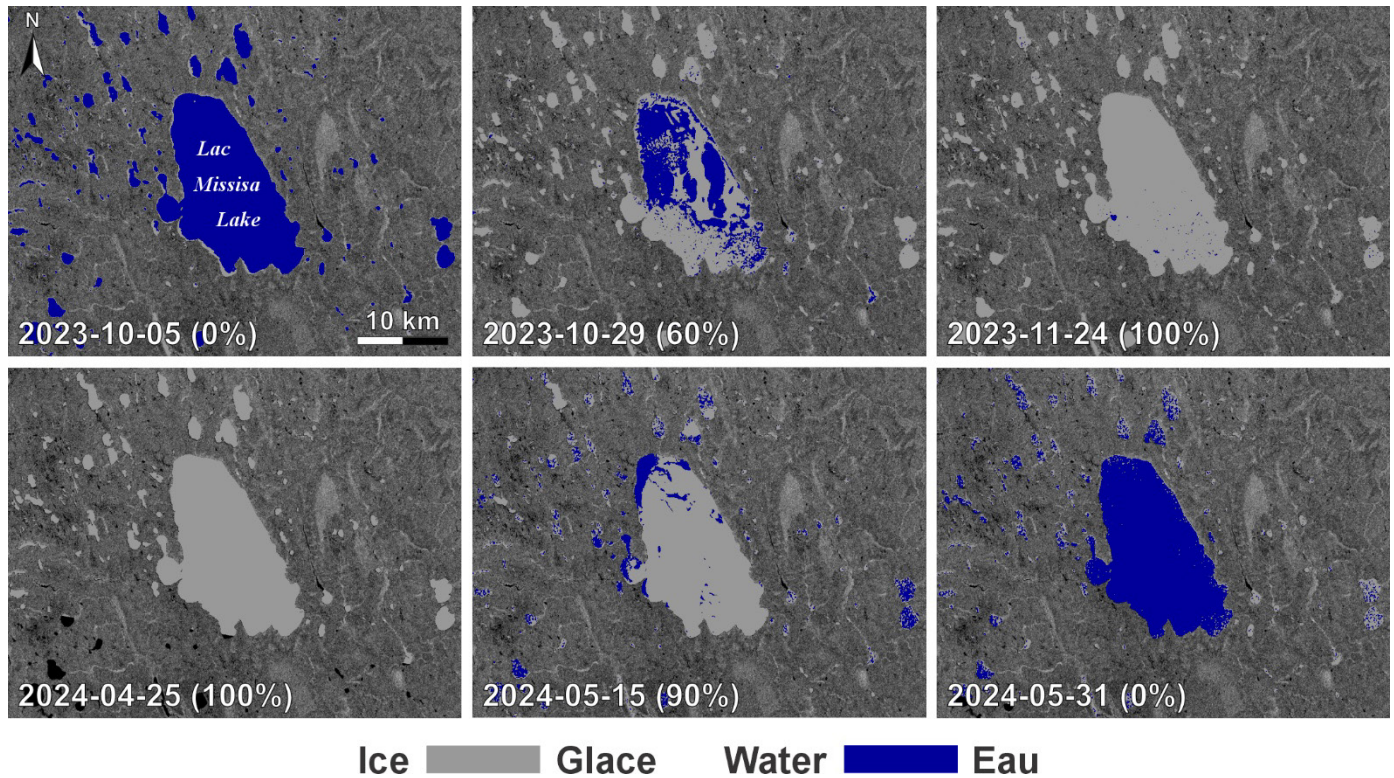


Fig. 1. Lake ice extent maps showing a section of the Ring of Fire assessment area centered on Missisa Lake (52°19' N, 85°12' W). The maps derive from RADARSAT Constellation Mission images acquired during the 2023 freeze-up season (October to November) and 2024 breakup season (April to May). The percentages represent the lake ice concentrations for Missisa Lake. RADARSAT Constellation Mission Imagery © Government of Canada (2023, 2024). RADARSAT is an official mark of the Canadian Space Agency.

of freeze-up and of breakup and, by extension, the duration of both the ice-on and ice-off seasons as well as ice freeze-up / breakup / duration anomalies.

Figure 1 shows six lake ice extent maps for a section of the Ring of Fire assessment area that centers on Missisa Lake (52°19' N, 85°12' W). These maps were produced by applying our classification models to selected RCM images acquired during the 2023 freeze-up season (October to November) and the 2024 breakup season (April to May). Additionally, the lake ice concentrations for Missisa Lake are presented, i.e. the percentage following each date. Lake ice concentrations for the neighbouring lakes are available but not shown for clarity's sake.

According to Figure 1, the freeze-up and breakup dates for Missisa Lake were 24 November 2023 and 31 May 2024, respectively. As such, the duration of the 2023-2024 ice-on season for this lake is estimated to be 189 days. The smaller lakes surrounding Missisa Lake appear to have an earlier freeze-up date

(see the map for 2023-10-29) while their breakup date is more in line with the one for Missisa Lake.

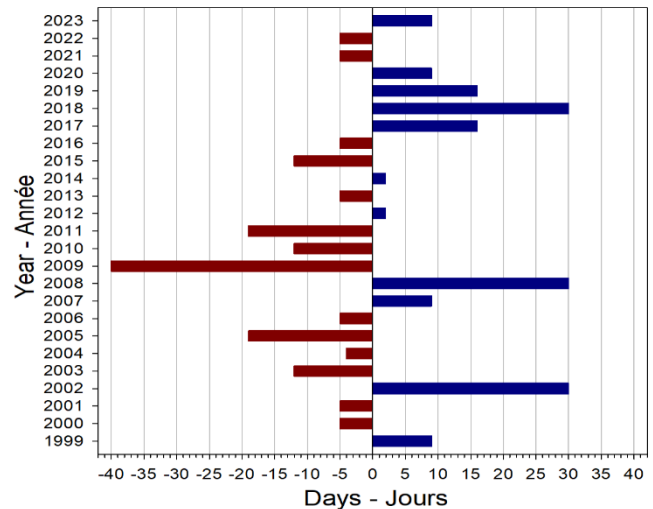


Fig. 2. Plot showing ice-duration anomalies for Missisa Lake from 1999 to 2023. Blue and red bars represent years where, respectively, the ice duration is longer and shorter than the long-term average of 187 days. Data source: ECCC/CIS.

For many users, including those involved with regional assessments, the value of lake ice extent information increases as its timespan expands. To illustrate this point, we have elected to augment the information captured in Figure 1 with information derived from data provided by the Canadian Ice Service (CIS) of Environment and Climate Change Canada (ECCC). For weather forecasting and climate modelling purposes, CIS analysts apply a variety of EO images to visually interpret the weekly extent of ice on up to 136 Canadian lakes including Missisa Lake. Their observation record for Missisa Lake goes back to 15 December 1998 and was applied here to create the ice-duration anomaly plot shown in Figure 2. The labels on the y-axis correspond to the freeze-up season. As such, the year 2023 represents the 2023-2024 ice-on season and matches the time period associated with Figure 1. It is beyond the scope of this text, our objective, and our expertise, to analyze the information available in Figure 2 in detail. However, we would like to share one obvious, to us, unexpected, observation. That is, from one year to another the duration of the ice-on season for Missisa Lake can vary by as much as 70 days (e.g. from 2008 to 2009). The long-term anomalies in terms of freeze-up dates and breakup dates could be plotted in a similar manner and provide additional insight into the phenology of ice cover on Missisa Lake.

Conclusions and next steps

Information about lake ice extent supports decision-making in the context of regional assessments because it may reveal natural and man-made changes in environmental conditions. As a result of interconnections, such changes may then alter health, cultural, social and economic circumstances.

Thanks to their unique imaging capacity, SAR satellites make excellent tools to collect lake ice extent information. Our approaches facilitate the automated extraction of lake ice extent information from SAR satellite images and are therefore more sustainable than methods that engage image analysts.

A quantitative evaluation of the accuracy of our ice vs. water classification models is in progress. Ground conditions that are known to reduce classification accuracy during freeze-up include the presence of

wind shadows and very thin new ice. Similarly, the presence of wet snow, pooling water and high winds creates challenges for the classification of ice vs. water during breakup.

For more information, please contact: Joost.vanderSanden@NRCan-RNCan.gc.ca

References

- [1] Leppäranta, M., 2015. *Freezing of Lakes and the Evolution of Their Ice Cover*. Springer-Verlag, Heidelberg etc., 301 p.
- [2] Thompson, A., 2015. Overview of the RADARSAT Constellation Mission. *Canadian Journal of Remote Sensing*, Vol. 41, No. 5, pp. 401-407.
- [3] Geldsetzer, T. and J.J. van der Sanden, 2013. Identification of polarimetric and non-polarimetric C-band SAR parameters for application in the monitoring of lake ice freeze-up, *Canadian Journal of Remote Sensing*, Vol. 39, No. 3, pp. 263-275.
- [4] Geldsetzer, T., J.J. van der Sanden, and B. Brisco, 2010. Monitoring Lake Ice during Spring Melt using RADARSAT-2 SAR, *Canadian Journal of Remote Sensing*, Vol. 36, No. 2, pp. S391-S400.

Indicator 5. Terrestrial Water Storage

Relevance to the ROF assessment priorities

Water and aquatic ecosystems in Ontario's Ring of Fire (ROF) region are essential to local Indigenous peoples for cultural, ecological, and practical reasons. Water is regarded as sacred and life-giving, central to teachings, ceremonies, and responsibilities of stewardship, while lakes, rivers and wetlands support vital food sources such as fish, wild rice, and waterfowl that sustain traditional livelihoods. The waterways also function as travel routes, connecting communities and reinforcing identity and heritage. The ROF has a water-rich landscape, crossed by six major rivers, and local communities depend on these rivers for drinking water, transportation, and food. The region overlaps with the Hudson Bay Lowlands, one of the world's largest peatland complexes and a critical global carbon sink. In their natural waterlogged state, these oxygen-poor wetlands slow decomposition, allowing peat to accumulate and store vast amounts of carbon. However, shifts in water balance—caused by drainage, road building, mining, climate change, or altered river flow—threaten this equilibrium. Drying exposes peat to oxygen, accelerating decomposition and releasing carbon dioxide, while excessive flooding can increase methane emissions from microbial activity. Both processes risk transforming the Lowlands from a carbon sink into a greenhouse gas source, undermining climate regulation and triggering feedback loops that intensify warming and hydrological change. Beyond carbon storage, the wetlands regulate water flow, filter pollutants, and sustain biodiversity, making them critical for local environmental health. Indigenous communities have voiced strong concerns that mining in the Ring of Fire could contaminate water, disrupt wetlands, and damage fish and wildlife habitats, endangering their culture, food security, and future generations.

Given these risks, monitoring and quantifying terrestrial water storage (TWS) and its variability have become increasingly important. Understanding how water is stored and redistributed across the landscape is central not only to hydrology and climatology but also to ecology, water resource management, and socio-economic planning.

Previous studies highlight the value of TWS assessments in tracking long-term water balance, evaluating climate impacts, and informing sustainable management strategies [1].

The Gravity Recovery and Climate Experiment (GRACE) satellite mission, launched in 2002, provides a unique opportunity to monitor monthly changes in TWS by tracking variations in Earth's gravity field [2]. Because TWS reflects the combined contributions of groundwater, soil moisture, surface water, snow, and ice, it offers valuable insight into how different water components interact within ecosystems. GRACE-based studies have successfully captured groundwater depletion, basin-scale water balance, evapotranspiration, snow and ice changes, floods, droughts, and vegetation responses, demonstrating GRACE's broad relevance for hydrology and climate research. Building on this foundation, we characterize the TWS climatology for the ROF region using GRACE observations from 2002 to 2024, with the aim of improving understanding of regional water cycle dynamics.

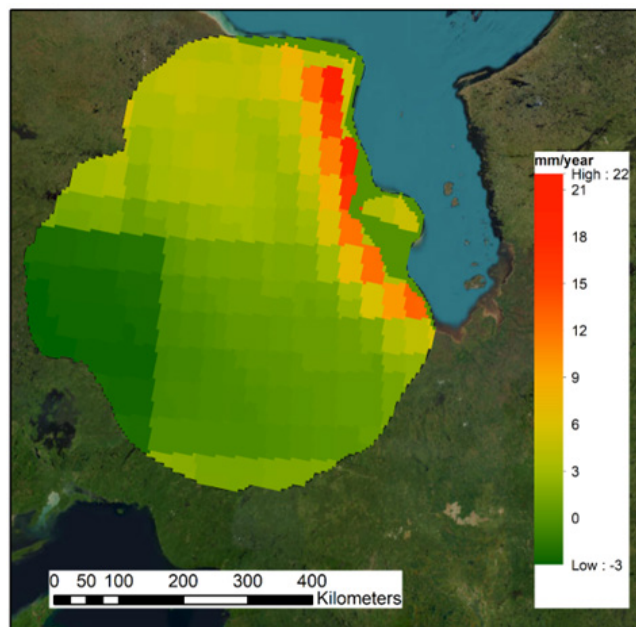


Fig. 1. Trends of TWS (Sen's slope) for Terrestrial Water Storage in 2002–2024 in the Ring of Fire region, derived from GRACE mascon products. The trend is overlaid on an ArcGIS basemap.

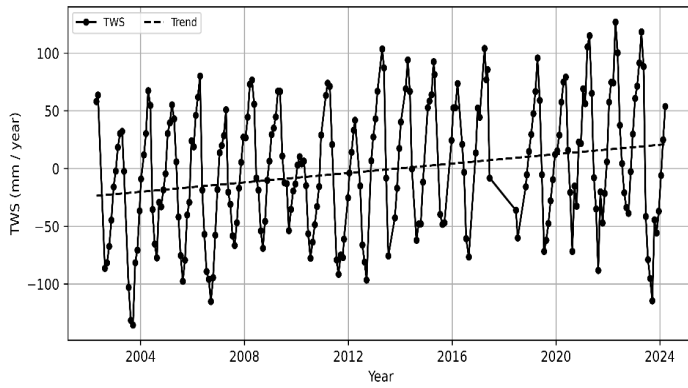


Fig. 2. Monthly averaged TWS in the Ring of Fire region for 2022-2024.

Methodology

TWS for the ROF region in northern Ontario was derived from the GRACE and GRACE Follow-On (FO) satellite missions for the period April 2002–March 2024. Monthly datasets were obtained from three data processing centers: the Center for Space Research, University of Texas [3], the Goddard Space Flight Center [4], and the Jet Propulsion Laboratory, NASA [5]. To reduce uncertainties associated with individual processing strategies, ensemble means were used to produce a consolidated dataset. The resulting fields were reprojected to a 5 km spatial resolution grid in Lambert Conformal Conic projection, and values were extracted for the ROF study area using a regional mask.

Indicator Definition

Eight variables were calculated from the monthly TWS time series to characterize the climatology of the study area [6]. These include:

1. M_{\max} and M_{\min} – the months of maximum and minimum TWS occurrence, indicating seasonal timing of peak and lowest water storage.
2. σ_{\max} and σ_{\min} – the standard deviations of M_{\max} and M_{\min} across years, representing interannual variability in seasonal timing.
3. ΔTWS – the maximum seasonal variation range of TWS, calculated as the mean difference between M_{\max} and M_{\min} over 2002–2024.
4. COV – the coefficient of variation of ΔTWS , representing interannual variability in seasonal amplitude.
5. Sen’s slope – the trend of the monthly TWS

time series, representing long-term change.

6. p-value – the statistical significance of Sen’s slope, based on a two-tailed test.

The Sen’s slope was spatially mapped for the ROF region (Fig. 1). The other seven variables were derived using the monthly averaged TWS across the ROF region owing to space constraints of this report.

Early Results

The ROF region exhibits a pronounced seasonal cycle in TWS, with maximum storage (M_{\max}) occurring around April, driven by snow accumulation, and minimum storage (M_{\min}) around August, following peak evapotranspiration in the summer. The average transition duration between M_{\max} and M_{\min} is ~ 4.5 months (Fig. 2). Across the record, M_{\max} ranges from March to June ($\sigma_{\max} = 0.7$ months), while M_{\min} occurs between July and October ($\sigma_{\min} = 0.9$ months).

The mean seasonal amplitude (ΔTWS) is 155 ± 32 mm, ranging from 87.9 to 232.7mm, with the largest variations (>200 mm) along the southern shore of Hudson Bay and the smallest (<100 mm) in the Winisk Watershed region (Fig. 3). The coefficient of variation of ΔTWS is 0.21, indicating moderate interannual variability.

Over the 22-year study period, Sen’s slope analysis

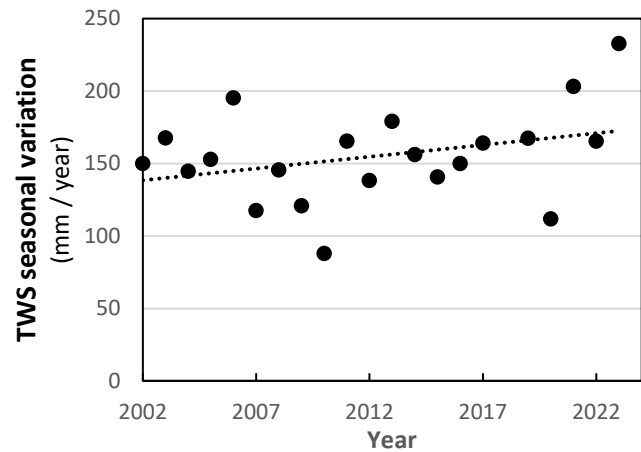


Fig. 3. Seasonal variation of TWS from 2002 to 2024 (21 years, by excluding 2024).

shows a long-term TWS increase averaging 2.03 mm yr^{-1} ($p < 0.001$), with a spatial gradient from shoreline to inland: the largest positive trends reach 22 mm yr^{-1} along the bay shore, while negative trends down to -3 mm yr^{-1} occur inland (Fig. 1). Elevated shoreline trends may partly reflect uncertainty in GRACE

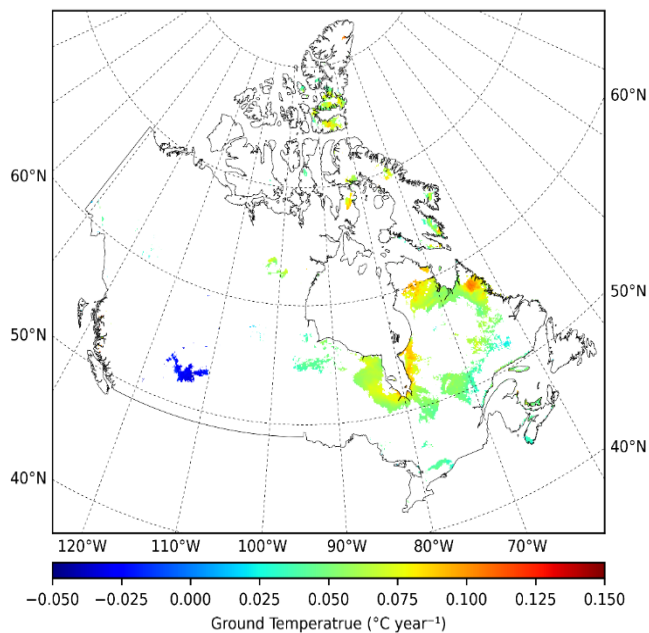


Fig. 4. Sen's slope of simulated ground temperature from 1950 to 2023 using the EALCO model, used to interpret TWS variations. Significant positive trends are observed in the Hudson Bay Lowlands.

products.

Seasonal TWS variability (Δ TWS) exhibits a weak positive trend of 1.3mm yr^{-1} ($p=0.2$), which may be linked to climate-driven increases in air and ground temperatures that enhance evapotranspiration and extend the growing season, thereby amplifying seasonal water storage oscillations, as shown in Fig. 4.

Although the results suggest modest long-term storage gains, interpretation must account for uncertainties associated with post-glacial rebound and the coarse spatial resolution of GRACE. Nonetheless, integrating GRACE-derived TWS anomalies with land surface models and hydrometric records provides a valuable framework for monitoring water availability and hydrological resilience in the ROF, where in situ observations remain sparse.

Conclusions and Next Steps

GRACE and GRACE-FO observations reveal a pronounced seasonal cycle of terrestrial water storage (TWS) in Ontario's Ring of Fire, with a mean amplitude of $155 \pm 32\text{mm}$ and maxima/minima in April and August, respectively. Sen's slope analysis

indicates a modest long-term increase of $\sim 2.03\text{mm yr}^{-1}$. Leakage errors and post-glacial rebound effects may cause uncertainties in the results. While seasonal variability shows only a weak upward trend ($\sim 1.3\text{mm yr}^{-1}$), the results highlight the value of GRACE-based monitoring for characterizing hydrological dynamics in this data-sparse, peatland-dominated region.

For more information, contact:

Liming.He@NRCan-RNCan.gc.ca,

Shusen.Wang@NRCan-RNCan.gc.ca.

References

- [1] X. Shi *et al.*, "Quantifying the long-term changes of terrestrial water storage and their driving factors," *Journal of Hydrology*, vol. 635, p. 131096, May 2024, doi: 10.1016/j.jhydrol.2024.131096.
- [2] B. D. Tapley, S. Bettadpur, M. Watkins, and C. Reigber, "The gravity recovery and climate experiment: Mission overview and early results," *Geophysical Research Letters*, vol. 31, no. 9, 2004, doi: 10.1029/2004GL019920.
- [3] H. Save, S. Bettadpur, and B. D. Tapley, "High-resolution CSR GRACE RL05 mascons," *JGR Solid Earth*, vol. 121, no. 10, pp. 7547–7569, Oct. 2016, doi: 10.1002/2016JB013007.
- [4] B. D. Loomis, K. E. Rachlin, and S. B. Luthcke, "Improved Earth Oblateness Rate Reveals Increased Ice Sheet Losses and Mass-Driven Sea Level Rise," *Geophysical Research Letters*, vol. 46, no. 12, pp. 6910–6917, 2019, doi: 10.1029/2019GL082929.
- [5] F. W. Landerer *et al.*, "Extending the Global Mass Change Data Record: GRACE Follow-On Instrument and Science Data Performance," *Geophysical Research Letters*, vol. 47, no. 12, p. e2020GL088306, 2020, doi: 10.1029/2020GL088306.
- [6] S. Wang and J. Li, "Terrestrial Water Storage Climatology for Canada from GRACE Satellite Observations in 2002–2014," *Canadian Journal of Remote Sensing*, vol. 42, no. 3, pp. 190–202, May 2016, doi: 10.1080/07038992.2016.1171132.

Indicator 6. Caribou Lichen Availability

Relevance to the ROF assessment priorities

One of the key assessment priorities for healthy environmental relationships is “wildlife and wildlife habitat, including species at risk, migratory birds, and fish and fish habitat” as outlined in the “Terms of Reference for the Regional Assessment in the Ring of Fire (ROF) Area.” Among the wildlife species at risk in Canada, the boreal population of woodland caribou was officially assessed as threatened under the Species at Risk Act in 2003, with this status confirmed in 2014. Caribou are vital to Canada for ecological, cultural, and economic reasons. They serve as a keystone species, reflecting the health of ecosystems, and hold significance in Indigenous cultures, ways of life, and economies. The ROF assessment area comprises six caribou ranges (see Figure 1): five boreal caribou ranges (Missisa, Ozhiski, Nipigon, Pagwachuan, and James Bay) and one migratory caribou range (Hudson Bay Lowland).

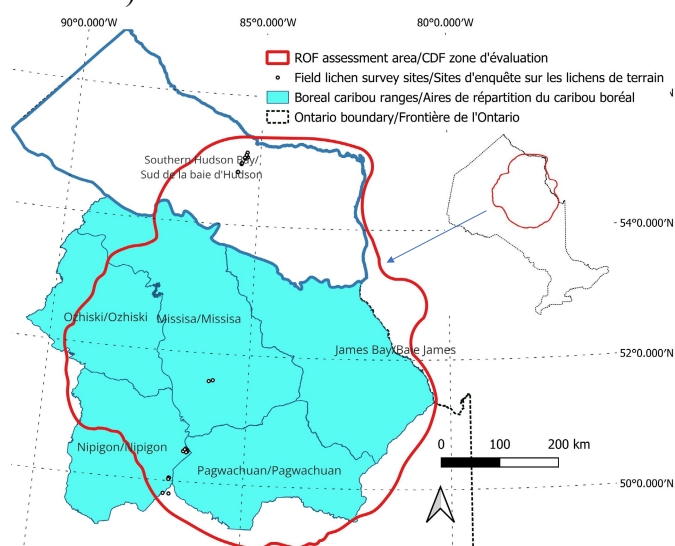


Fig. 1. Boreal and migratory caribou ranges that mostly overlap with the ROF assessment area in Northern Ontario. The inserted figure shows the location of the ROF area in Ontario, Canada. Also plotted are the locations of our field lichen surveys conducted in 2020 and 2022.

Several factors, including habitat quality and loss, hunting, predation, diseases and parasites, industrial development, extreme weather events, climate change, and their interactions, can threaten caribou

populations. In most cases, the exact causes of caribou declines remain unclear and likely differ across regions and over time. To evaluate these causes and develop effective recovery strategies, comprehensive information on all factors is crucial. These factors tend to be complex and quantifying them requires multiple indicators. For example, boreal caribou habitat can be divided into seven distinct seasons: year-round, calving, summer, rutting, winter, late winter, and migration. A scientific review by Environment Canada revealed that, for winter range alone, various types of critical habitat have been identified in studies across the ROF area and surrounding regions. For instance, in the Hudson Bay Lowland and James Bay Lowland, caribou prefer dense coniferous forests, wetlands, and mature coniferous forests with lichens. They also favor habitats with sandy soils, islands, and forests of black spruce, spruce-larch, and jack pine-spruce in the Lake Nipigon area. A recent dietary study by Thompson et al. confirmed that lichens are vital for boreal caribou populations in northern Ontario, making up 76% and 79% of their diet during fall and winter, respectively. However, it's important to acknowledge that not all these habitat types have sufficient lichen. Relying solely on broad habitat categories can be imprecise and misleading. Using detailed lichen availability maps will improve the identification of critical winter habitats and support land management efforts. Therefore, caribou lichen availability should be a key indicator in the ROF assessment priority “wildlife and wildlife habitat.”

Methodology

When developing a methodology for mapping lichen availability using satellite imagery, we must consider the scale effects resulting from the varying sizes of the study objects and satellite imagery.

(1) The size of a caribou's range. As shown in Figure 1, a boreal caribou range typically covers thousands of square kilometers. The simplest way to cover these caribou ranges in the ROF area is to use coarse-resolution satellite data, such as Advanced Very-High-Resolution Radiometer (AVHRR). Since 1980, the AVHRR sensor has provided daily global

coverage with a ground resolution of approximately 1.1 km. Alternatively, we can use moderate-resolution satellite data, such as Landsat, which has a ground resolution of 30m and a revisit period of 16 days since the 1980s. To cover all these caribou ranges in the ROF area, we mosaic hundreds of Landsat scenes from adjacent years. These medium- and coarse-resolution satellite data are freely available and openly accessible, with extensive historical records for trend analysis.

(2) The sizes of various lichen distribution patterns to be mapped are identified. Based on literature and our field surveys across Canada, we categorize lichen distribution into three main patterns: scattered, patchy, and carpet. For the scattered pattern, terrestrial lichens are primarily distributed by individual plants, with a crown diameter usually less than a few millimetres. The length and width of a lichen patch are measured in centimetres, while those of a lichen carpet can span meters or more. Considering these size ranges and the tendency of terrestrial lichens to be located beneath trees and shrubs, direct mapping using medium- or coarse-resolution satellite images would likely yield poor accuracy. Conversely, drone images with a spatial resolution of < 2 cm allow us to distinguish lichen patches or carpets from trees, shrubs, and other plants. Down-looking plot photos with a resolution of < 1 mm would be most effective for identifying lichen species at the individual plant level, providing additional information on the availability of lichens. Since caribou must dig through snow to access lichen, and energy balance considerations suggest scattered lichen is not a significant food source, our focus is on mapping lichen patches and carpets.

(3) The scales of caribou winter habitat selection. Caribou's winter habitat choice occurs at multiple scales: they primarily choose areas for predator avoidance at the landscape level; at the land patch level, they focus on lichen abundance; and at the feeding site level, they prefer locations with easier access, such as areas with shallow snow and proximity to tree trunks and shrub branches. The feeding sites are typically on the scale of decimeters to meters, as indicated by the lichen craters formed during winter feeding. Land patches tend to be on the scale of dozens of meters, while landscapes are on the scale of kilometers. A map with a spatial

resolution of 30m is thus suitable for identifying land patches with abundant lichen. Therefore, for land use planning and impact assessment, maps with a 30-meter resolution may be better than those with a coarser resolution of 500-1000 meters.

We developed an upscaling method for mapping caribou lichen availability that addresses these scale effects. Specifically, the method includes four steps: (1) develop a large ground truth database from field plot photos and drone footage [1], which have suitable spatial resolution for distinguishing lichen patches and carpets, (2) scale up from <2 cm resolution ground truth data to 30m resolution Landsat-derived lichen cover maps using high resolution satellite images (e.g., WorldView at a 0.5m ground resolution), to cover all caribou ranges in the ROF area [2], (3) converting the Landsat-derived lichen cover maps into the status maps of lichen availability using criteria for ecological lichen classification, supporting critical habitat identification and land use planning, and (4) detecting historical changes in lichen availability using Landsat time series and harmonization methods, to support the ROF regional impact assessment [4].

Indicator definition and early results

An effective environmental indicator should meet three criteria: it should be relevant to the object assessed, practical for implementing management options, and feasible to monitor. According to these criteria, we proposed to define the caribou lichen availability indicator as the area of the good and moderate lichen availability classes in a caribou range.

Figure 2 displays the status of caribou lichen availability across the Ozhiski caribou range. Land areas with no or low lichen availability dominated the range. In contrast, land with good or moderate lichen availability made up only 0.01% or 2.29% of the range, respectively. We hypothesize that certain development projects could lead to a 3% loss of the Ozhiski caribou range. If this loss had occurred in areas with good and moderate lichen availability, it could be devastating to the caribou population. However, using the broader habitat type of conifer forest, which covers 75% of the range, the impact might seem less severe. Of course, the locations with good or moderate lichen availability were widely

distributed in the caribou range, whereas development projects would be more concentrated. As such, a few development projects are unlikely to affect all areas with good or moderate lichen availability. Nevertheless, this example shows that relying on broad habitat types can be inaccurate and misleading. Explicit lichen availability maps would be a better alternative.

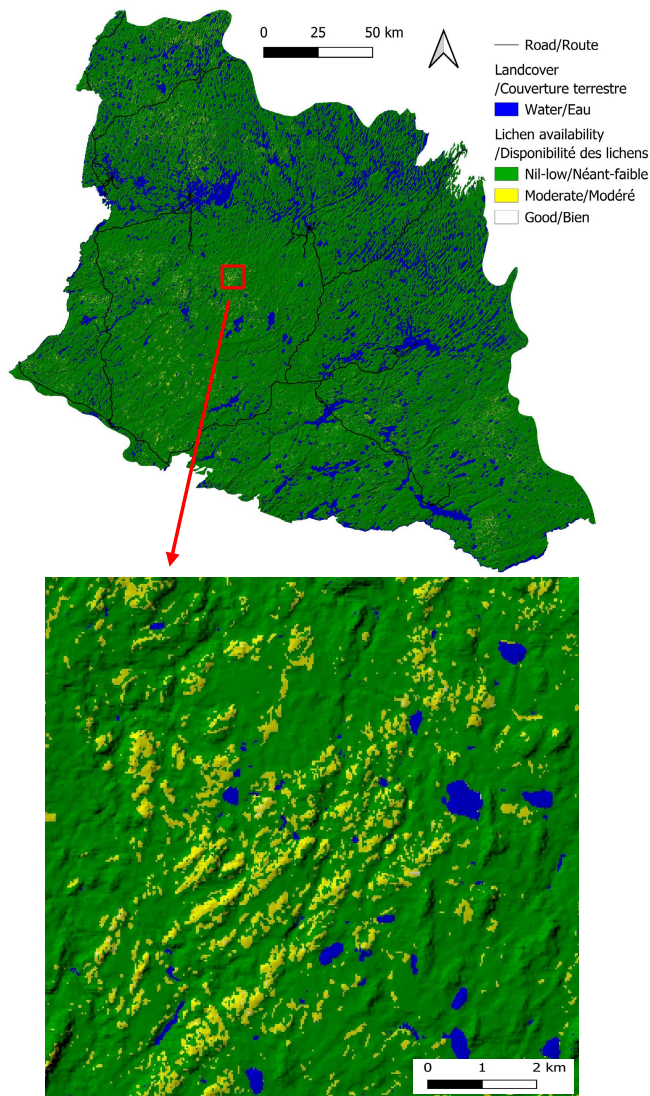


Fig. 2. A circa-2020 current condition map of lichen availability for the Ozhiski caribou range in Ontario, Canada. Also included is a zoomed-in 10 km by 10 km map. The 3-D effect was added to show the topography of the area using DEM data.

Conclusions and next steps

Caribou is a priority species at risk in the ROF area. Our results show that the use of broad habitat types (e.g., mature conifer forest) can be imprecise and misleading, and lichen availability is a more suitable indicator for caribou winter range. Currently, land

areas with moderate to good lichen availability account for <3% of the Ozhiski caribou range. Therefore, these areas with moderate to good lichen availability should be a priority for habitat conservation.

For the next steps, we will finalize the status maps and identify trends in the lichen availability for caribou ranges in the ROF area. We will also analyze the relationship between lichen availability and broad habitat types and assess the cumulative effects on lichen availability for caribou ranges in the ROF area. The results will be included in our upcoming plain-language open-file report, with the data released on the Open Science and Data Platform. For more information, contact: Wenjun.Chen@NRCan-RNCan.gc.ca.

References

- [1] J. Lovitt, G. Richardson, K. Rajaratnam, W. Chen, S. G. Leblanc, L. He, S. E. Nielsen, A. Hillman, I. Schmelzer, and A. Arsenault, "A new U-net based convolutional neural network for estimating caribou lichen ground cover from field-level digital photographs," *Canadian Journal of Remote Sensing*, vol. 48, no. 6, pp. 849–872, 2022, <https://doi.org/10.1080/07038992.2022.2144179>
- [2] S. Jozdani, D. Chen, W. Chen, S.G. Leblanc, C. Prévost, J. Lovitt, L. He, B.A. Johnson, "Leveraging Deep Neural Networks to Map Caribou Lichen in High-Resolution Satellite Images Based on a Small-Scale, Noisy UAV-Derived Map", *Remote Sensing*, vol. 13, pp. 2658, 2021, <https://doi.org/10.3390/rs13142658>
- [3] L. He, W. Chen, S.G. Leblanc, J. Lovitt, A. Arsenault, I. Schmelzer, R.H. Fraser, R. Latifovic, L. Sun, C. Prévost, H.P. White, D. Pouliot, "Integration of multi-scale remote sensing data for reindeer lichen fractional cover mapping in Eastern Canada," *Remote Sensing of Environment* vol. 267, pp. 112731, 2021, <https://doi.org/10.1016/j.rse.2021.112731>
- [4] G. Richardson, A. Knudby, K. Millard, K., W. Chen, A tool for global and regional Landsat 7 and Landsat 8 cross-sensor harmonization. *Geocarto International*, vol. 40, no. 1, pp. 2538108, 2025, <https://doi.org/10.1080/10106049.2025.2538108>

Indicator 7. Beaver Engineering

Relevance to the ROF assessment priorities

The North American beaver (*Castor canadensis*) can be found in aquatic environments across Ontario where its leafy vegetation forage occurs. Beaver populations started recovering in the early 1900s after being devastated by overexploitation during the fur trade that began in the 1600s and played an important role in Canadian history [1]. Where beavers build dams across stream channels, they have a major impact on ecosystems by creating ponds that retain water and sediment, removing vegetation for food and building material, and forming biodiverse wetland habitats. The engineering activities of beavers also buffer against drought, attenuate high flows during floods, and provide firebreaks and shelter from large wildfires, thus offering a nature-based solution for mitigating the effects of climate change.

The *Terms of Reference for the Regional Assessment in the Ring of Fire Area* includes *Healthy Environmental Relationships* as a main priority. Knowledge of the spatial distribution of beaver wetlands and how they vary through time is important for addressing all components listed under this priority: *water and river systems (including flows), wildlife and wildlife habitat, climate change adaptation, and biodiversity*. Although beaver ponds can be frequently observed in satellite images across the 312,000 km² Assessment Area (Figure 1) that covers portions of the Hudson Bay Lowlands and Boreal Shield, little information is available describing their regional distributions and long-term changes [2].

Methodology

Beavers are traditionally surveyed in northern climates using aerial surveys to visually detect the presence of food caches constructed by beavers in the fall next to their lodges. However, aerial beaver cache surveys are expensive and not practical for large regions such as the Ring of Fire Assessment Area. Information related to beaver harvesting is collected annually by the Ontario government for several hundred trapline areas within the Assessment

Area, but this may not provide a reliable measure of beaver population changes. Each beaver trapline covers only a portion of the larger landscape and the number of harvested animals will vary due to factors other than population size, such as changing pelt prices, trapping effort, and regulations. Potential beaver dam and pond density may also be estimated using habitat suitability models, although their predictions will be region-specific and may not strongly agree with actual beaver presence.



Fig. 1. Area within the southern portion of the Ring of Fire Assessment area (84.89°W, 49.96°N) where a high density of beaver dams, lodges, and ponds can be observed in high resolution (~0.5 m) satellite data.

To overcome these limitations for tracking beaver activity across large regions, we developed a method to measure long-term beaver pond changes using satellite remote sensing. The locations of all new and abandoned beaver dams are identified using high resolution imagery to distinguish satellite-mapped water bodies that were created or at least modified by beavers [3]. This approach uses the condition of beaver ponds (i.e., either filled or drained) as an indicator of the presence of a beaver colony that is actively maintaining a dam, since dams will degrade and most ponds gradually drain after they are abandoned. The method was demonstrated over a 5,000 km² region of the coastal Hudson Bay Lowlands in Manitoba, which required digitizing 1,714 beaver dams using high-resolution (~0.5m) satellite data. Since digitizing all current and older

beaver dams would be impractical over the entire Ring of Fire Assessment Area, we are modifying this beaver pond mapping approach.

Our new method will use a machine learning model to distinguish beaver ponds based on their unique spatial and temporal properties that can be measured using optical and Synthetic Aperture Radar (SAR) satellite data, satellite-based vegetation and land cover products, and digital elevation models (Figure 2). The model is being developed using more than 15,000 observations of beaver ponds and non-beaver ponds from four training regions covering the range of conditions found within the Assessment Area. It will then be used to classify all 238,000 long-term water bodies in the Assessment Area that are at least 0.5 ha and located within 200m of a stream. A validation of the predictions will be conducted using randomly sampled regions that were not used to develop the model.

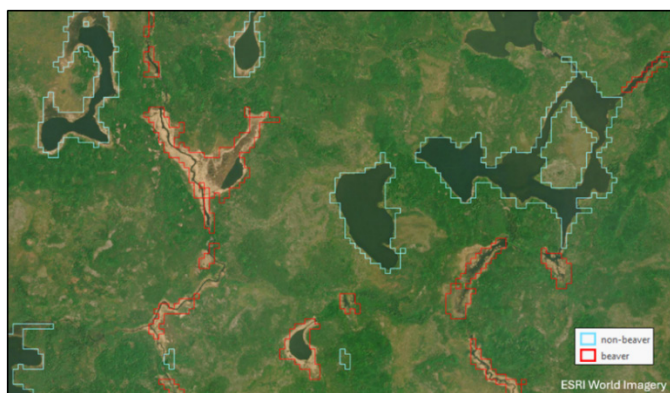


Fig. 2. Example predictions of beaver-engineered ponds (red outlines) and non-engineered ponds (blue outlines) from a random forests machine learning model (87.56°W, 53.24°N). In this satellite image, beaver ponds are mostly in a drained state by comparison to ponds in Figure 1, suggesting that they are not currently occupied by beaver colonies.

Indicator definition and early results

The first indicator that can be derived using this mapping approach characterizes the large-area, spatial variation of beaver ponds. The results from a preliminary version of our model that predicts 49,000 long-term beaver ponds are shown aggregated within 20 km hexagonal bins in Figure 3. This output represents the density of water bodies > 0.5 ha that have been flooded by beaver engineering at least once since 1985 and indicates the suitability of different regions in the Assessment Area for

supporting beaver populations. Beaver pond density should also be related to the multiple benefits of beaver wetlands that were described previously.

A second indicator will track annual variability of these beaver ponds over a 37-year period (1985-2021) to reveal any regional shifts in beaver engineering activity. Yearly summer surface water area for each pond will be derived using a technique designed to measure smaller water bodies with 30m resolution Landsat satellite data [4]. The annual area of each pond can also be expressed as a percentage of its long-term (1985-2021) maximum area, and then a threshold is applied (e.g., 30%) to predict the presence of a colony that is maintaining a beaver dam. For example, the full beaver ponds in Figure 1 would suggest that colonies are present compared to the drained ponds in Figure 2. The total ponded area and the number of likely colonized ponds for each year will be aggregated in the same manner as in Figure 3 and presented as animations and long-term trends.

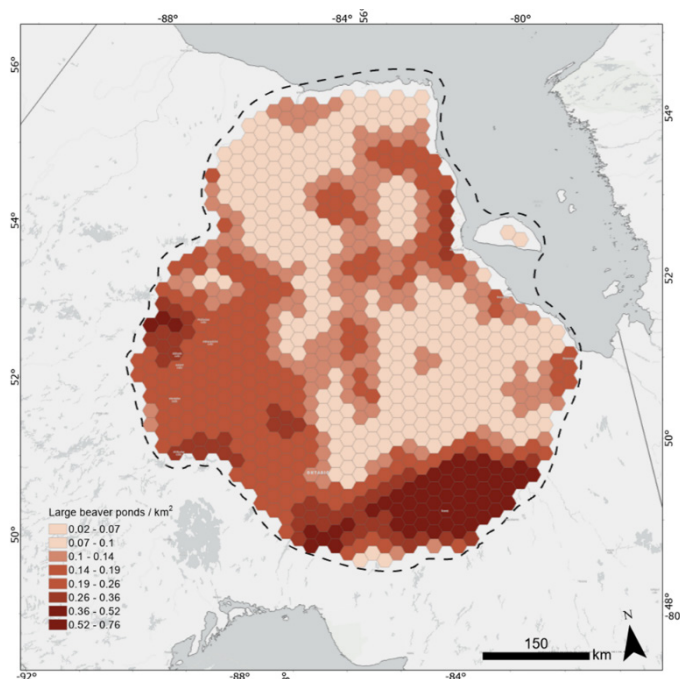


Fig. 3. Preliminary predictions of beaver pond density within the 312,000 km² Ring of Fire Assessment Area in Ontario. This measures the occurrence of beaver ponds that were flooded at any time during the period 1985-2021.

Conclusions and next steps

Beavers create ponds and wetlands through their engineering activities that provide multiple ecosystem services and climate change resilience in

the Ring of Fire Assessment Area. Our satellite-based method for annual mapping of beaver pond surface water area will offer new information on the spatial and temporal variability of beaver activity throughout this region. Development, application, and validation of the model is anticipated to be completed in 2026.

This research is being conducted in collaboration with Ian Olthof and Darren Pouliot at Environment and Climate Change Canada, and Glen Brown at the Ontario Ministry of Natural Resources. For more information, contact: Robert.Fraser@NRCan-RNCan.gc.ca

Bay Lowlands, Canada using sub-pixel Landsat Analysis Remote Sens. Environ. 113895.

References

- [1] Rosell F and Campbell-Palmer R. 2022 Beavers: Ecology, Behaviour, Conservation and Management; Oxford University Press: Oxford, UK
- [2] Abraham, K.F., McKinnon, L.M., Jumeau, Z., Tully, S.M., Walton, L.R. and Stewart, H.M. (lead coordinating authors and compilers). 2011. Hudson Plains Ecozone+ Status and Trends Assessment. Canadian Biodiversity: Ecosystem Status and Trends 2010, Technical Ecozone+ Report. Canadian Councils of Resource Ministers, Ottawa, ON. xxi + 445 pp.
- [3] Fraser R H, Olthof I and Berezanski D 2024 Large multi-decade beaver ponding changes in the subarctic Hudson Bay Lowlands, Canada observed using satellite remote sensing Environ. Res. Lett. 19(4):044061.
- [4] Olthof I and Fraser R H 2024 Mapping Surface Water Dynamics (1985-2021) in the Hudson

Indicator 8. Land Cover

Relevance to the ROF assessment priorities

The Ring of Fire region in northern Ontario, Canada, represents one of the country's most ecologically and geologically significant landscapes. Situated within the Hudson Bay Lowlands—home to vast peatlands, boreal forests, and freshwater systems—this remote and largely undeveloped area is now facing mounting pressure from proposed mining and infrastructure development [1]. In this context, land cover mapping and classification play a critical role in informing impact assessments, which are essential for evaluating how future projects may affect ecosystems, water resources, and local communities. Accurate and up-to-date land cover information provides the necessary spatial foundation to assess potential disturbances, quantify habitat loss, monitor cumulative effects, and guide decision-making toward more sustainable and responsible development pathways [2].

Boreal forests and expansive peatland wetlands play distinct yet interconnected ecological roles throughout this landscape. The boreal forest, part of one of the largest intact forest systems globally, is essential for maintaining biodiversity, supporting species at risk such as woodland caribou, and providing long-term carbon storage. Equally important are the region's wetlands, particularly the vast peatlands of the Hudson Bay Lowlands, which act as major carbon sinks and play a crucial role in hydrological regulation and biodiversity. Mapping and classifying these ecosystems with high spatial and thematic accuracy is critical for detecting change, understanding cumulative impacts, and informing sustainable land-use decisions. These efforts support effective conservation strategies and ensure that industrial development does not compromise the long-term health and function of these sensitive ecological systems.

Land cover maps were traditionally created through field surveys, where experts manually recorded vegetation types and land use characteristics. While offering high local accuracy, this method is resource-intensive and impractical for large or remote regions like the Ring of Fire. With

the advancement of satellite remote sensing, land cover classification has shifted to analyzing Earth Observation (EO) imagery, which captures surface characteristics over broad areas. These data can now be processed using machine learning algorithms and accessed through cloud platforms, enabling efficient, scalable, and repeatable mapping.

Recent advances in remote sensing technologies, machine learning, and cloud computing offer transformative opportunities for land cover mapping in such a remote and ecologically sensitive region. These innovations support not only baseline assessments but also long-term environmental monitoring—crucial for understanding the cumulative impacts of industrial development in areas like the Ring of Fire. Importantly, the integration of land cover data into environmental decision-making can also empower Indigenous communities, who demonstrate stewardship roles across much of the region. When combined with Indigenous knowledge systems, geospatial data becomes a powerful tool to support land governance, safeguard cultural values, and guide development in ways that reflect community priorities.

Methodology

Sentinel-2 data were used as the main source of satellite data for land cover mapping in this study, given their sufficient spatial resolution relative to the size of existing land cover classes in the region and rich spectral information. With 13 spectral bands at 10m, 20m, and 60m resolutions, Sentinel-2 enables accurate discrimination of key land cover types, such as boreal forests, wetlands, peatlands, and surface water. The availability of visible, near-infrared (NIR), and shortwave infrared (SWIR) bands enhances the detection of vegetation characteristics, moisture conditions, and land disturbances—essential for mapping and monitoring the complex ecosystems in this remote and ecologically sensitive region. Its 5-day revisit cycle ensures consistent temporal coverage, which is particularly valuable given the frequent cloud cover and short snow-free season in northern Ontario. Moreover, Sentinel-2 data is openly accessible through platforms like the

Copernicus Open Access Hub and Google Earth Engine, making it an affordable and scalable solution for ongoing environmental monitoring, impact assessments, and supporting Indigenous-led stewardship in the Ring of Fire assessment area.

For this study, Sentinel-2 bands with spatial resolution of 10m and 20m, from May to September, were used, with the 20m bands resampled to 10m resolution to create median composites. Additionally, images with cloud coverage below 5% were selected to ensure data quality and reliability.

An advanced deep learning (DL) model has been developed at the Canada Centre for Remote Sensing (CCRS) [3] to produce large-scale (provincial-scale) land cover maps. The method employs a two-step classification framework that integrates both machine learning and DL techniques, effectively addressing the limitations of training data that often constrain conventional DL models in large-scale land cover mapping.

Indicator definition and early results

The first indicator that can be derived using the proposed approach is the characterization of land cover categories and their spatial distribution in the study area. In regions like the Ring of Fire, characterized by vast boreal landscapes, significant wetland coverage, and increasing development interest, land cover indicators play a critical role in tracking environmental change, informing cumulative impact assessments, and guiding land-use planning. Figure 1 illustrates the land cover map of the Ring of Fire area, covering an area of approximately 319,000 km², derived from Sentinel-2 imagery using the proposed approach. This land cover map has 10 land cover classes, following the Level-1 North American Land Change Monitoring System (NALCMS) [4], compatible with the previous effort of large-scale land cover mapping in CCRS. Note that the two classes of snow/ice and cropland were removed in this sub-region of Ontario, as there are no permanent ice and snow classes in the region, and there is no agricultural activity as well.

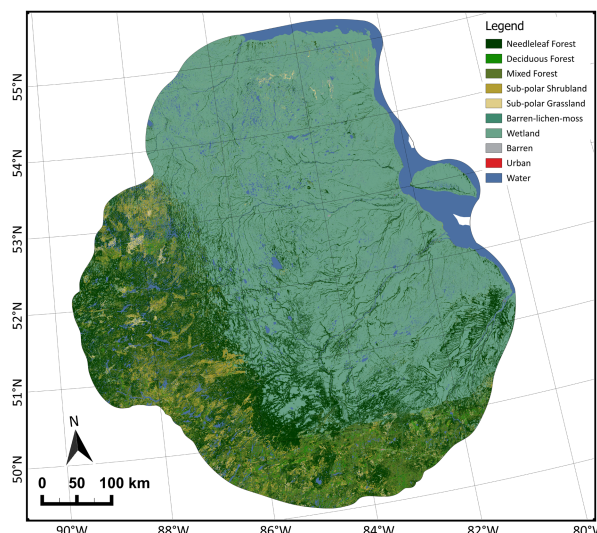


Fig. 1. The land cover map in the Ring of Fire Assessment Area in Ontario with a spatial resolution of 10m obtained from Sentinel-2 multi-spectral data.

As demonstrated, the two classes of forest (particularly needleleaf forest) and wetland are dominant land cover categories in the study area. Figure 2 illustrates the distribution of land cover classes within the study area.

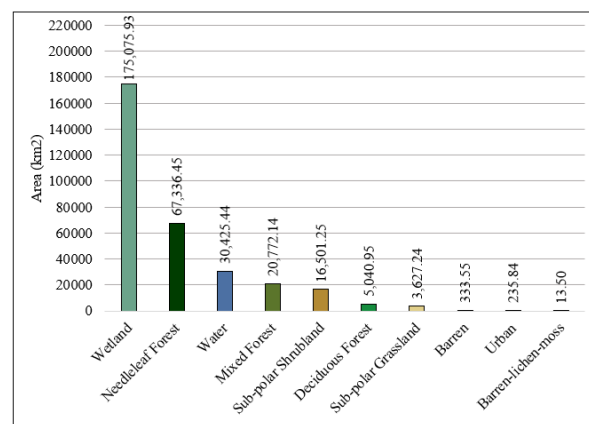


Fig. 2. The distribution of 10 land cover classes within the Ring of Fire assessment area.

As illustrated in Figure 2, wetlands constitute the largest proportion, occupying approximately 175,075 km², followed by needleleaf forest (67,336 km²) and water bodies (30,425 km²). Mixed forest (20,772 km²), sub-polar shrubland (16,501 km²), deciduous forest (5,04 km²), and sub-polar grassland (3,627 km²) represent smaller but ecologically significant. The three classes of barren areas (333.55 km²), urban areas (235.84 km²), and barren-lichen-moss (13.50 km²) are the less dominant classes in the

study area. Figure 3 and 4 shows the masks of two dominant land cover classes in the study area.

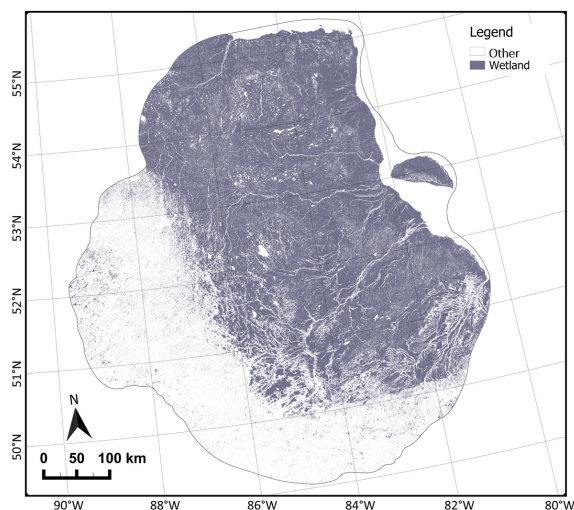


Fig. 3. Wetland mask showing the extent of wetland versus non-wetland area in the Ring of Fire assessment area.

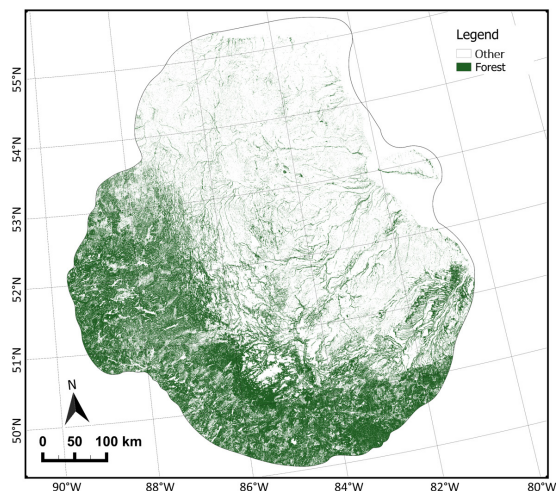


Fig. 4. Forest mask showing the extent of forest versus non-forested area in the Ring of Fire assessment area.

As illustrated in Figures 3 and 4, the dominance of wetlands and forests underscores the ecological importance of this region and its role in supporting biodiversity, hydrological functions, and carbon storage

Conclusions and next steps

Our results illustrate the distribution of existing land cover types in the study area, where both wetlands and forests are identified as the dominant land cover categories. The 2023 land cover map developed in

this study provides a valuable reference point for detecting future changes and monitoring landscape dynamics as development activities proceed in the region. Analysis of the current landscape reveals that wetlands and forested areas are the predominant land cover types, underscoring the ecological sensitivity and carbon storage significance of this region.

As a next step, an annual land cover change analysis will be conducted using satellite time series data to assess spatial and temporal shifts in land cover patterns. The time series analysis will use the resulting land cover map from this study as a reference point to track annual changes and trends over this area. This will involve the use of multi-temporal satellite observations and change detection algorithms to identify patterns of disturbance or conversion. The change detection analysis is especially important in the context of the anticipated infrastructure, mining, and road development projects in the Ring of Fire area. Land cover should be considered a complementary environmental indicator in ongoing cumulative effects assessments, environmental impact assessments (EIAs), and regional planning frameworks. These insights will inform regulatory processes, support Indigenous-led environmental stewardship, and contribute to evidence-based policy development for sustainable resource management in Northern Ontario. For more information, contact: fariba.mohammadimanesh@nrca-nrcan.gc.ca

References

- [1] C. Burton and C. Chetkiewicz, "Terrestrial ecological monitoring: A review and recommendations for northern Ontario's Ring of Fire," *Unpubl. Rep. WCS Can. Alta. Innov. Futur. Httpsdoi Org10*, vol. 13140, 2015.
- [2] E. F. Lambin and H. J. Geist, *Land-use and land-cover change: local processes and global impacts*. Springer Science & Business Media, 2008..
- [3] F. Mohammadimanesh, "Large Scale Land Cover Mapping in Ontario, Canada, Using a Deep Learning Framework," *IEEE J. Sel. Top. Appl. Earth Obs. Remote Sens.*, 2025.
- [4] M. Pasos, "NALCMS — The North American Land Change Monitoring System," Commission for Environmental Cooperation.

Indicator 9. Vegetation Cover and Density

Relevance to the ROF assessment priorities

The ROF encompasses “a vast expanse of intact boreal forest and peatland complexes that, despite being inhabited for thousands of years, remain largely undisturbed by large-scale industrial development activities” [1]. Vegetation is essential to environmental health in the ROF by providing habitat, impacting permafrost stability, controlling flooding, and supporting one of the world's largest carbon sinks. Like much of northern Canada, natural disturbances such as forest fires, together with climate change, can impact vegetation in the ROF. Mineral exploration and mining will also modify vegetation cover due to new roads, mines, and infrastructure [2]. As such, it is important to have data on current and historical vegetation cover, density, and productivity to ensure future development is sustainable. We describe here an approach based on satellite mapping and machine learning that addresses this data need and can complement site-specific surveys and traditional knowledge.

Methodology

Forest inventory and airborne surveys are a primary source of data for monitoring vegetation in managed forests and inhabited regions [3,4]. However, such data are not available for the ROF due to the absence of managed forests and the large percentage (54%) of vegetated wetlands. Satellite based land cover maps can identify vegetated land but do not provide information on the status and trends in vegetation canopy cover, density or productivity.

Here, indicators of vegetation quantity and condition are derived from physical variables that describe vegetation structure and productivity (Table 1). They are mapped at 20m to 30m resolution using multi-year time series of satellite imagery. These variables are applicable across all vegetated land cover classes and have been designated as ‘essential’ by UN climate, biodiversity and agriculture expert panels [5,6,7]. FCOVER generalizes the concept of crown

cover to land cover other than forests and maps within land cover class variation in vegetation cover. LAI provides a land cover independent measure of vegetation density that includes both overstory and understory vegetation. FAPAR provides an upper limit on vegetation productivity widely used to model annual carbon uptake.

The Landscape Evolution and Forecasting Toolbox (LEAF) is used to produce monthly maps for the entire ROF and seasonal time series by applying physics-based machine learning algorithms to relate light reflected from the surface across multiple wavelengths to each variable [8]. LEAF uses machine learning algorithms to map FCOVER, LAI, and FAPAR from cloud-free 30m resolution Landsat and 20m resolution Sentinel-2 satellite imagery. These algorithms offer comparable accuracy (better than 10% for FCOVER and FAPAR and 20% for LAI) to on-the-ground measurements across North America, including sites bordering the ROF [9,10], and temporal stability sufficient to detect changes as little as 2.5% per year [11].

Table 1. Mapped vegetation variables.

Variable	Definition	Relevance
FCOVER	fraction of vegetation cover	How much of the land is vegetated?
LAI	Leaf area index	How dense is the vegetation?
FAPAR	Fraction of absorbed light for photosynthesis	What is the potential vegetation productivity?

Indicator definition and early results

Site-specific and regional indicators for vegetation quantity and condition are based on the maximum annual value of FCOVER and LAI, and, for FAPAR, the integrated value during June, July, and August. LEAF is used to map FCOVER, LAI, and FAPAR for all cloud-free satellite measurements, starting from 30m Landsat imagery since 2013,

supplemented by 20m Sentinel 2 imagery since 2016, in the site. These data can provide up to daily sampling but only the maximum site average value is used as a quantity indicator to reduce sensitivity to the number of clear sky observations each year. Maximum annual FCOVER and LAI (e.g., Figure 1) are used as quantity indicators, and the integrated annual FAPAR is used as a condition indicator.

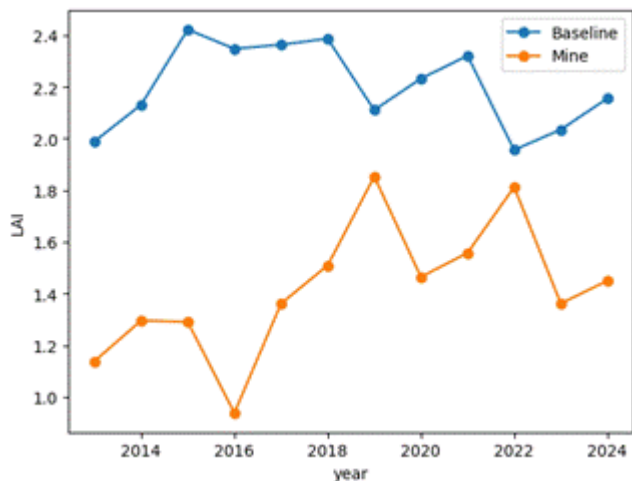


Fig. 1. Maximum annual LAI within 100m of infrastructure at the Eagles-Nest project (mine) initiated in 2012 compared to baseline conditions in an external 100m buffer. Increased LAI over mine reflects regenerating exploration corridors.

Regional indicators for the entire ROF are derived using monthly rather than daily time series of each variable to reduce the impact of clouds on temporal sampling. The maximum FCOVER and LAI are estimated for each pixel (Figure 2). FAPAR is not shown as it is very similar to FCOVER. LAI and FCOVER are highest in the coastal and southern regions of the study area. Land cover-specific vegetation condition indicators are also derived for each sub-watershed. These are defined as the average maximum annual LAI and average total FCOVER for a given land cover class (e.g., Figure 3). LAI and FCOVER are lowest in the Hudson Bay lowlands, where forests correspond to low-density taiga, and greatest in the southern ROF, where forests correspond to productive softwoods.

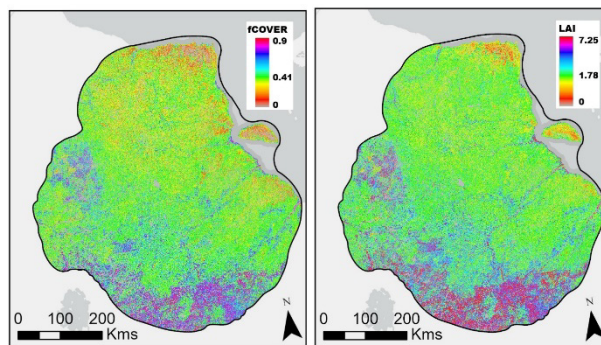


Fig. 2. Maximum FCOVER (left) and maximum LAI (right) for 2023 mapped at 20m resolution from Copernicus Sentinel-2 imagery using the CCRS LEAF-Toolbox.

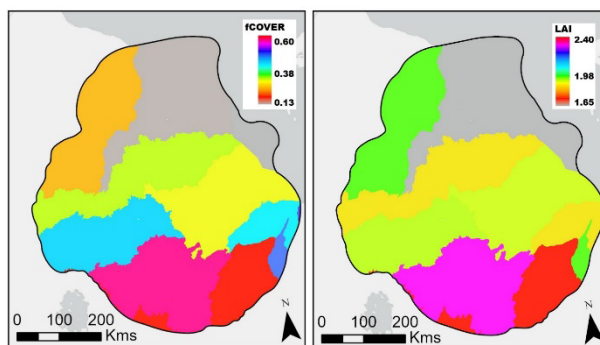


Fig. 3. Average conifer maximum FCOVER (left) and maximum LAI (right) for 2023 during 2023 conifer forest pixels for sub-watersheds in ring of fire. Similar indicators are produced for other land cover classes.

Conclusions and next steps

Vegetation provides many ecosystem services within the ROF. Climate and land use change will impact vegetation. Indicators of historical and current vegetation quantity and condition can be reliably mapped using free and open satellite imagery with minimal in-situ surveys. The work presented provides indicators of regional spatial patterns and local temporal trends. Forthcoming results will provide regional assessments of temporal trends for 15 15-year extent recommended for climate studies. For more information, contact: Richard.Fernandes@NRCan-RNCan.gc.ca

References

1. IAAC (2025). Terms of reference for a regional assessment in the Ring of Fire area. Accessed at <https://iaac-aeic.gc.ca/050/evaluations/proj/80468?culture=en-CA> on August 21, 2025.
2. Alberta Biodiversity Monitoring Institute. 2014. ABMI Science Letters: Human Footprint in Alberta. Accessed at: <https://abmi.ca/publication/364.html> on August 21, 2025.
3. Burton, Cole & Chetkiewicz, Cheryl-Lesley. (2015). Terrestrial Ecological Monitoring: A review and recommendations for Northern Ontario's Ring of Fire. 10.13140/RG.2.1.4468.6568.
4. Alberta Biodiversity Monitoring Institute. 2017. Regional Mapping of Vegetation Structure for Biodiversity Monitoring Using Airborne Lidar Data. Available at: <https://abmi.ca/publication/466.html>
5. GEOGLAM. (2022). Full EAV table | AgVariables. Accessed at <https://agvariables.org/> on August 12, 2025.
6. WMO (World Meteorological Organization) (2022). The 2022 GCOS Implementation Plan (GCOS-244). World Meteorological Organization. Accessed at <https://library.wmo.int/records/item/58104-the-2022-gcos-implementation-plan-gcos-244> [WMO e-Library](https://library.wmo.int/records/item/58104-the-2022-gcos-implementation-plan-gcos-244) on August 12, 2025.
7. Navarro, L.M., Fernández, N., Guerra, C., Guralnick, R., Kissling, W.D., Londoño, M.C., et al. (2017). Monitoring biodiversity change through effective global coordination. *Curr. Opin. Environ. Sustain.*, 29, 158–169.
8. Fernandes, R., Baret, F., Brown, L., Canisius, F., Dash, J., Djamai, N., Hong, G., Kalimpalli, S., Latifovic, R., MacDougall, M., Shah, H., Weiss, M., Harvey, K., & Sun, L. (2021). LEAF Toolbox: A software for environmental and remote sensing data analysis. <https://github.com/rfernand387/LEAF-Toolbox/wiki> (Accessed January 2025)
9. Fernandes, R., Brown, L., Canisius, F., Dash, J., He, L., Hong, G., Huang, L., Le, N. Q., MacDougall, C., Meier, C., Darko, P. O., Shah, H., Spafford, L., & Sun, L. (2023). Validation of simplified level 2 prototype processor Sentinel-2 fraction of canopy cover, fraction of absorbed photosynthetically active radiation, and leaf area index products over North American forests. *Remote Sensing of Environment*, 293, Article 113600. <https://doi.org/10.1016/j.rse.2023.113600>
10. Fernandes, R., Djamai, N., Harvey, K., Hong, G., MacDougall, C., Shah, H., & Sun, L. (2024). Evidence of a bias-variance trade-off when correcting for bias in Sentinel-2 forest LAI retrievals using radiative transfer models. *Remote Sensing of Environment*, 305, Article 114060. <https://doi.org/10.1016/j.rse.2024.114060>
11. Djamai, N., Fernandes, R., Sun, L., Hong, G., Brown, L., Morris, H., & Dash, J. (2025). On the consistency and stability of vegetation biophysical variables retrievals from Landsat-8/9 and Sentinel-2. *ISPRS Journal of Photogrammetry and Remote Sensing*, 224, 329–347. <https://doi.org/10.1016/j.isprsjprs.2025.04.006>

Indicator 10. Permafrost

Relevance to the ROF assessment priorities

The Ring of Fire (ROF) region experiences seasonal thawing/freezing, and some areas contain permafrost that remains frozen throughout the year. Ground thawing/freezing and permafrost have significant impacts on roads and buildings, water flow and water levels, plant types and growth, soil decomposition and greenhouse gas emissions, particularly in the peat-rich Hudson Bay Lowlands (HBL). Ground thermal conditions vary from place to place, and they are changing with climate warming. However, our knowledge of permafrost is limited. Figure 1 shows the current Canada permafrost map around the ROF region. The map divided the landmass into five zones representing different probabilities or areal percentages of permafrost. It has no information about the exact locations, conditions, and potential changes with climate warming. Such a coarse map is not practically useful for local communities and regional assessments.

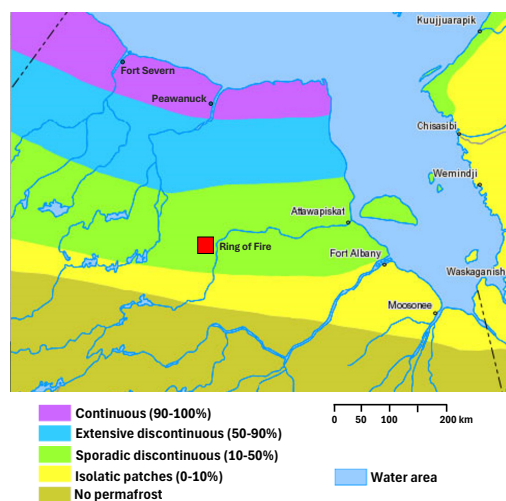


Fig. 1. The permafrost distribution in ROF assessment area based on the current Canada permafrost map [1].

In this study, we developed a new method to model and map ground temperature, thawing/freezing, and permafrost across the HBL at 30m resolution and their potential changes with climate from 1950 to 2100.

Methodology

The method is based on the Northern Ecosystem Soil Temperature (NEST) model, which simulates ground temperature dynamics based on heat conduction, including the effects of snow and thawing/freezing of water [2]. Snow is a major factor causing variations in ground thermal conditions at the landscape-scale. The model uses a parameter (F_{snow}) to represent variations in snow redistribution due to wind. The F_{snow} for each grid cell is estimated based on snow disappearance dates, which are mapped from satellite data at 30m resolution (see Indicators 1 and 2). We also accounted for lateral heat flows among grid cells, including the effects of water bodies [3]. Ground thawing/freezing depths and permafrost are determined based on the modelled ground temperature conditions. To efficiently map ground temperature at 30m resolution, we ran the model for various possible F_{snow} values, vegetation and ground conditions over a small number of sites, then interpolated the model results to 30m grid cells based on their locations and local conditions. The climate data are from ERA5-Land. The land cover types and peat thickness are from Ian Olthof and Emily Ogden, respectively, in Environment and Climate Change Canada (personal communications). Leaf area index was calculated based on Fernandes et al. [4] (Indicator 9).

Early results

Figure 2 shows the mapped annual mean ground temperature at 0.5m depth averaged for the recent decade (2015-2024). The mean ground temperature increases from north to south mainly due to the gradient of air temperature. It also shows large local-scale variations due to the impacts of snow, vegetation and ground conditions. Figure 3 shows the mapped maximum summer thaw depth averaged for the recent decade in permafrost areas. The white color is for areas without permafrost. Continuous permafrost is mostly restricted to northern areas. Most of the ROF assessment areas have discontinuous or no permafrost. Summer thaw depth generally increases from north to south, but with

large local-scale variations. Figure 4 shows the mapped maximum winter freezing depth averaged for the recent decade. Areas with deep freezing depth usually contain permafrost. The winter freezing depth becomes shallower from north to south, with strong local variations.

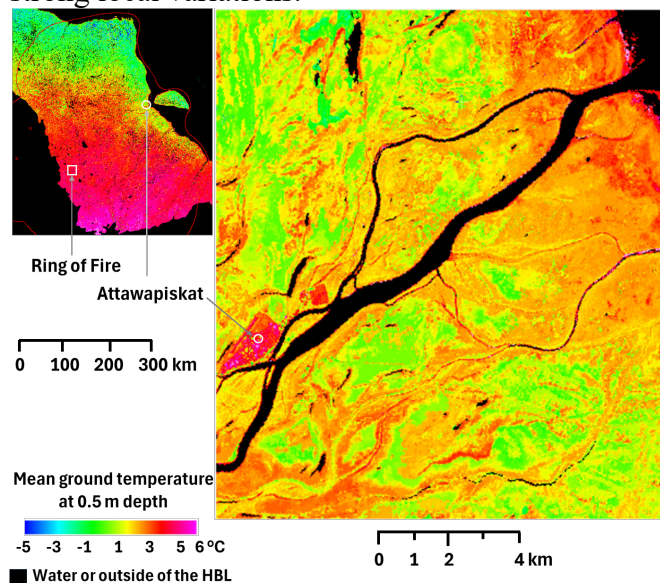


Fig. 2. Mapped annual mean ground temperature at 0.5m depth for the recent decade (2015-2024). The left panel shows a large part of the ROF impact assessment area in the HBL (its boundary is shown in the red curve), and the right panel is a small area around Attawapiskat as shown by a white circle.

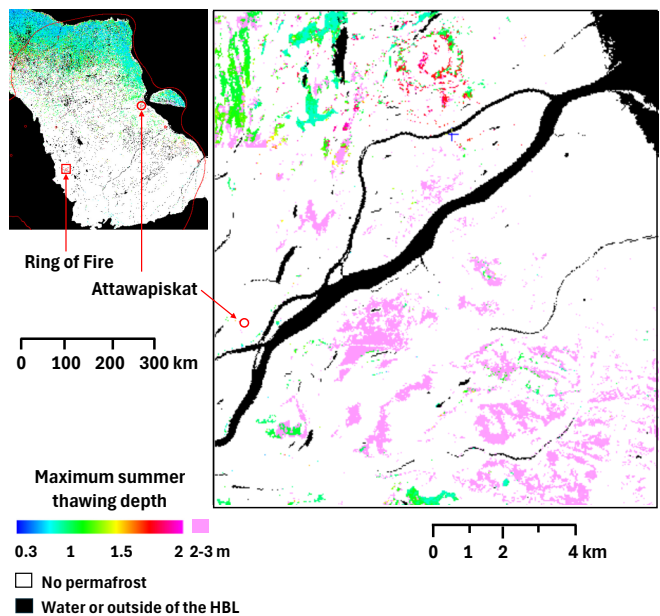


Fig. 3. Mapped maximum summer thaw depth in permafrost areas in the recent decade (2015-2024). The left panel shows a large part of the ROF impact assessment area in the HBL, and the right panel is a small area around Attawapiskat.

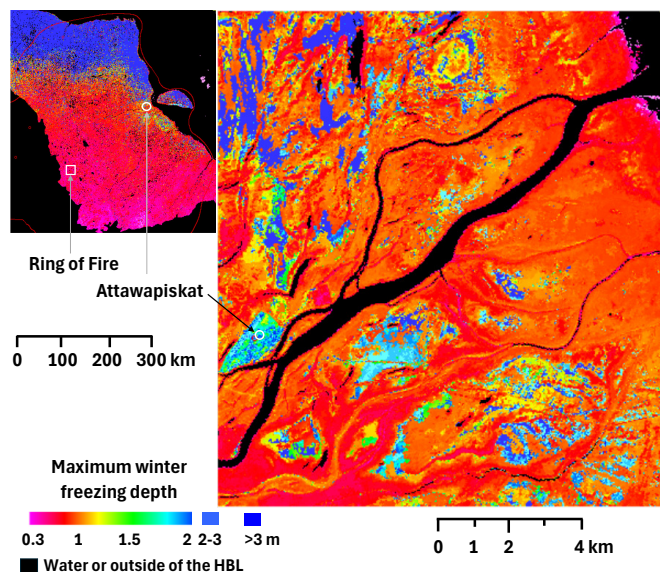


Fig. 4. Mapped maximum winter freezing depth averaged for recent decade (2015-2024). The left panel shows a large part of the ROF impact assessment area in the HBL, and the right panel is a small area around Attawapiskat. Areas with deep freezing depth usually contain permafrost.

Conclusions and next steps

Ground temperature, thawing/freezing, and permafrost have major impacts on the environment and communities in cold regions. Previous permafrost maps are too coarse for practical uses for local communities. We developed a new method to model and map ground thermal conditions and permafrost at 30m resolution. The results reveal both broad-scale variations with climate gradients and large fine-scale differences. Such spatially detailed information is important for land-use planning, infrastructure development, and climate adaptation strategies.

Our next steps are to analyze and validate the results based on observations, and to run the model under future climate change scenarios. We will also extend the products to cover the entire ROF assessment area. The results will be published later, and the data will be released on the Open Science and Data Platform.

For more information, contact: yu.zhang@NRCan-RNCan.gc.ca.

Acknowledgements

This study is funded by Park Canada Agency under the Hudson Bay-James Bay Biodiversity Conservation and Carbon Sequestration Initiative. This work is also supported by the following collaborators. Glen Brown of the Ontario Ministry of Natural Resources shared observations of climate, ground temperature, and permafrost data at multiple sites across the HBL region. Wendy Sladen and colleagues from the Geological Survey of Canada measured and compiled ground temperature data at multiple sites in Wapusk National Park. Jesse Shirton and LeeAnn Fishback of Wapusk National Park provided much of the field data collected in their Park. Alison Cassidy, Karen Richardson, and Alice Yue from Parks Canada Agency collected near-surface ground temperature at 41 sites. Rich Russell, Russ Weeber, David Hope, and Kevin Hannah from the Canadian Wildlife Service also collected near-surface ground temperature at 32 sites. We are grateful for their efforts in deploying and retrieving the tiny temperature sensors in the field. Kara Webster and her Canadian Forest Service team provided valuable support and suggestions. We also thank Emily Ogden, Ian Olthof, and Taylor Biccum from Environment and Climate Change Canada for providing us with a land cover map, a peat thickness map, and a sub-pixel water fraction map over the HBL. Xiping Wang processed station climate data and assessed gridded climate data sets. Gang Hong generated a leaf area index map.

fraction of absorbed photosynthetically active radiation, and leaf area index products over North American forests. *Remote Sensing of Environment*, 293, 113600. doi: 10.1016/j.rse.2023.113600

References

- [1] Atlas of Canada, 6th Edition (archive version) (2009). Permafrost. Natural Resources Canada, Ottawa, Canada.
- [2] Zhang, Y., W. Chen, and J. Cihlar, et al. (2003). A process-based model for quantifying the impact of climate change on permafrost thermal regimes. *Journal of Geophysical Research*, 108, D22, 4695. doi: 10.1029/2002JD003354
- [3] Zhang, Y., G. Hong, and M. T. Bonney. (2024). Impacts of lateral conductive heat flow on ground temperature and implications for permafrost modeling. *Scientific Reports*. 14, 31595. doi: 10.1038/s41598-024-78901-6
- [4] Fernandes, R., L. Brown, F. Canisius, et al. (2023). Validation of simplified level 2 prototype processor Sentinel-2 fraction of canopy cover,

Indicator 11. Terrain Deformation

Relevance to the ROF assessment priorities

Terrain deformation occurs as a result of many different processes, some natural and some anthropogenic. Deformation of the ground may be vertical up or down, horizontal, or both, and it may be simple displacement in a single direction or a heterogeneous local reshaping of the terrain. Large-scale regional deformation occurs due to geological and seismic processes; small-scale, local deformation occurs due to ecological and geomorphological processes and human activities. Monitoring the amounts and patterns of ground deformation can help us map terrain stability, identify areas that are experiencing change, as well as help us understand the processes at work and the causes of change.

The Hudson Bay Lowlands are relatively flat terrain underlain by permafrost. The region experiences seasonal deformation of the ground due to the freeze-thaw cycle of water contained in the upper layers of soil (the active layer). The magnitude of the seasonal deformation is primarily related to drainage conditions. Over time periods of years, deformation will also occur as a result of long-term geomorphological processes, including slope movement due to gravity, the growth and collapse of ice-cored landforms, the development of thermokarst with permafrost thaw, thermokarst lake expansion, lake drainage due to changing subsurface water flows, and lake shoreline migration due to wind patterns and riparian processes. Human activities can also cause terrain deformation, such as ground subsidence due to underground mining or resource extraction, ground heaving due to the injection of air or fluids into the ground to extract resources, or construction that modifies drainage patterns, vegetation cover, and ground thermal conditions.

Terrain deformation information could be useful for several topics included in the Ring of Fire Regional Assessment priorities (<https://iaac-aeic.gc.ca/050/documents/p80468/158865E.pdf>). Under Healthy Environment Relationships, 'Peatlands and other unique environments' can be better understood through their deformation

behaviours, and 'Climate change adaptation' is supported by an understanding of local geomorphological processes, likely impacts, and knowledge of vulnerable areas. Terrain deformation is also intertwined with local drainage patterns and can therefore be a component of understanding 'Water and river systems including flows'.

Methodology

Satellite radar interferometry (InSAR) is a method that measures displacement of the Earth's surface from space with millimetre precision. The method uses exactly repeating radar acquisitions over an area and tiny differences in the phase cycles of the radar waves to measure differences in the position of the ground surface. These pixel-by-pixel phase differences can be converted to large-area maps of ground displacement¹. It has been used for all scales of terrain deformation monitoring including studies in permafrost terrain^{2,3,4}.

Ground displacement is measured in the radar line-of-sight (LOS) direction, which is movement towards or away from the radar satellite. In very flat terrain, this measurement can be reliably converted to vertical displacement, which is more intuitive for users to understand, but it is generally not used where slopes would complicate the displacement patterns and cause confusing results. Over large areas, which may be a mix of flat and sloping areas, terrain deformation is usually displayed as LOS displacement.

The level of detail in the deformation maps depends on the nature of the radar data and the processing. High levels of detail are possible with high-resolution radar data and expert data processing, although this is costly and therefore reserved for small areas undergoing complex change. Regional and national-scale monitoring uses large volumes of moderate-resolution data that is free and processed in automated systems⁵.

Indicator definition and early results

Figure 1 shows the summer terrain deformation trends over the Ring of Fire Regional Assessment Area measured using medium-resolution radar data from the Sentinel-1 satellite. The spatial resolution is ~20m, and the observation time period is the summer thaw seasons between 2017 and 2024. Strong reds and blues show areas with strong seasonal deformation trends. These are dynamic areas with either slopes or high ice and water contents. These areas could be vulnerable if water flows were diverted, contaminated, or reduced under climate warming or anthropogenic change. Cream/yellow colours are areas that are relatively stable, often rock or well-drained gravels and sands. These areas tend to be less sensitive and more resilient to change.

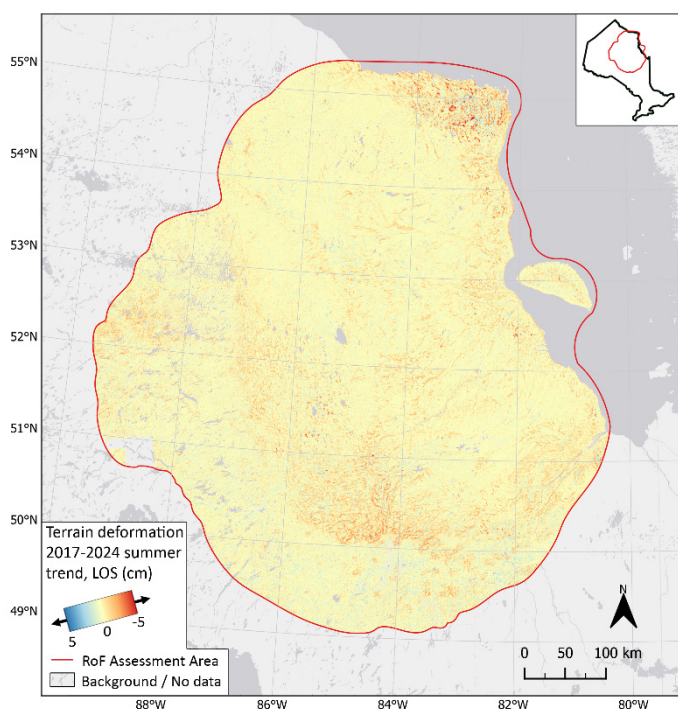


Fig. 1. Terrain deformation trend over summers 2017-2024 for the Ring of Fire Assessment Area, derived from Sentinel-1 radar interferometry.

Figure 2 shows an example of very high-resolution terrain deformation information from Polar Bear Provincial Park in the northeast corner of the Assessment Area, created using RADARSAT-2 data at 1m spatial resolution over the summer of 2023. The corresponding optical satellite image shows that certain deformation trends can be associated with different landforms and land cover types.

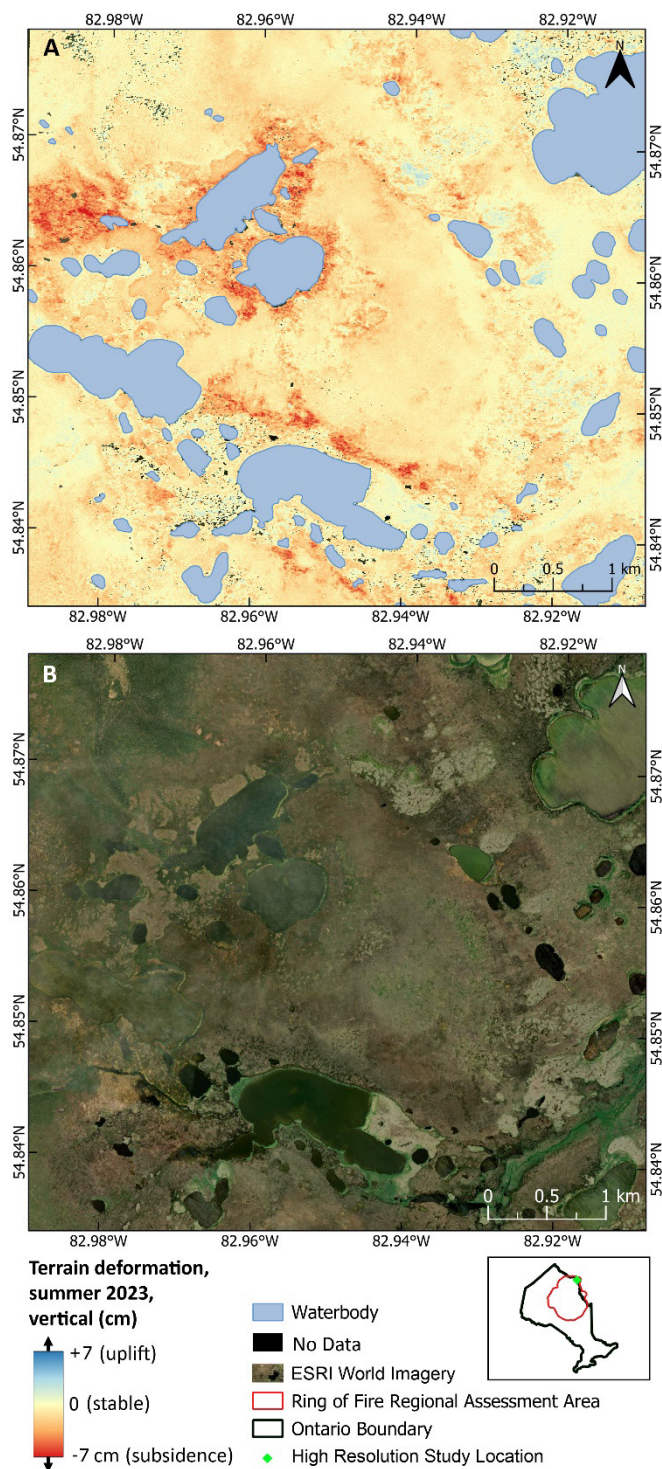


Fig. 2. A) Terrain deformation measured over summer 2023 at 1m resolution in Polar Bear Provincial Park using RADARSAT-2 Spotlight data. B) Corresponding optical satellite imagery.

Conclusions and next steps

Initial results show that it is possible to use radar interferometry to map terrain deformation over the

Ring of Fire Assessment Region. This enables us to identify areas that are naturally dynamic and vulnerable to change, versus areas that are stable and relatively inert. Rates and patterns of change help us understand the processes occurring at a location, which also helps us understand what the impacts of change might be. This can help in making decisions about where to permit development, what kinds of activities may be permitted at a site, and developing mitigation and conservation measures, for example, drainage control, infrastructure stabilisation or ground thermal management. After a site has been developed, mapping and monitoring terrain deformation can precisely identify areas that are experiencing change and quantify what the impacts of the development activities are. If mitigation measures have been implemented, terrain deformation information can be used to monitor the effectiveness of such measures. In summary, terrain deformation information can be useful for change detection and landscape management and conservation.

In the coming year, we will continue to develop and optimize methods for InSAR processing over the Hudson Bay Lowlands and northern Ontario, producing maps that can be used by communities and decision makers. The results of this work will be included in a second report. Where possible, final map products will be made publicly available via the Open Science and Data Platform.

For more information, contact:

naomi.short@nrcan-rncan.gc.ca

References

- [1] Gabriel, A., Goldstein, R. and Zebker, H. (1989). Mapping small elevation changes over large areas: differential radar interferometry. *Journal of Geophysical Research*, 94(B7): 9183-9191.
- [2] Short, N., Brisco, B., Couture, N., Pollard, W., Murnaghan, K. and Budkewitsch, P. (2011). A Comparison of TerraSAR-X, RADARSAT-2, and ALOS-PALSAR Interferometry for Monitoring Permafrost Environments, Case Study from Herschel Island, Canada, *Remote Sensing of Environment*, 115: 3491–3506. doi:10.1016/j.rse.2011.08012
- [3] Short, N., LeBlanc, A.-M., Sladen, W., Oldenborger, G., Mathon-Dufour, V. and Brisco, B. (2014). RADARSAT-2 D-InSAR for ground displacement in permafrost terrain, validation from Iqaluit Airport, Baffin Island, Canada. *Remote Sensing of Environment*. 141: 40-51, doi: 10.1016/j.rse.2013.10.016
- [4] Zwieback, S., Liu, L., Rouyet, L., Short, N. and Strozzi, T. (2024). Advances in InSAR analysis of permafrost terrain. *Permafrost and Periglacial Processes*, 35(4), 544-556. <http://doi.org/10.1002/ppp.2248>
- [5] Samsonov, S. and Feng, W. (2023). Deformation Retrievals for North America and Eurasia from Sentinel-1 DInSAR: Big Data Approach, Processing Methodology and Challenges. *Canadian Journal of Remote Sensing* doi:10.1080/07038992.2023.2247095.

Acknowledgement

First, we acknowledge that our study area, the Ring of Fire region, is located in a vast area of Northern Ontario that falls under the traditional territories of several Anishinaabeg and Cree Nations, including Aroland, Attawapiskat, Constance Lake, Eabametoong First Nation, Fort Albany, Ginoogaming, Kashechewan, Long Lake #58, Marten Falls, Missinabie Cree, Moose Cree, Neskantaga, Nibinamik, Webequie, and Weenusk First Nations.

The study is a part of the Earth Observation for Cumulative Effects (EO4CE) program, which is financially supported by the environmental assessment initiative announced in the 2018 federal budget and renewed in 2022. The Parks Canada Agency also provided funding for parts of this study as part of the Hudson Bay-James Bay Biodiversity Conservation and Carbon Sequestration Initiative.

Members of the Canada Centre for Mapping and Earth Observation management team played a vital role in preparing this report, including identifying the need, developing the plan, organizing the content, and providing editorial feedback. Sylvia Thomas and Peter White internally reviewed the report and offered numerous constructive comments. Alice Deschamps and Sylvian Leblanc coordinated the French Translation of this report and ensured scientific consistency between the English and French versions. In addition, a final proofread of the French text was completed by Raphaël Gendron.

Many partners from other federal government departments, provincial governments, and Indigenous communities have helped with this report. For example, Indigenous community members (e.g., David Hunter, Matthew Gull, Mike (Moose) Koostachin, Xavier Hunter, Abraham Hunter, Clinton Patrick, and Linda Friday of the Peawanuck Cree First Nation; Jack Moonias of the Marten Falls First Nation) and organizations (e.g., Four Rivers Environmental Services Group-Matawa Council, Mushkegowuk Council) guided and participated in our lichen field surveys in 2021 and 2022 in the ROF region. Sumac Geomatics, McMaster University, and World Wildlife Fund Canada also participated in our 2021 and 2022 field lichen surveys. Glen Brown of the Ontario Ministry of Natural Resources provided climate, ground temperature, and permafrost data measured at multiple sites across the Hudson Bay Lowlands. His team also completed two summers of field observations of landforms in Polar Bear Provincial Park to support the interpretation of terrain deformation maps. His field measurements, photographs, and insights into landscape composition were invaluable. Wendy Sladen and colleagues from the Geological Survey of Canada shared ground temperature data at multiple sites in Wapusk National Park. Jesse Shirton and LeeAnn Fishback of Wapusk National Park also provided ground temperature data collected in their park. Alison Cassidy, Karen Richardson, and Alice Yue from Parks Canada collected near-surface ground temperature at 41 sites. Rich Russell, Russ Weeber, David Hope, and Kevin Hannah from the Canadian Wildlife Service also collected near-surface ground temperature at 32 sites. We are grateful for their efforts in deploying and retrieving the temperature sensors in the field. Adam Collingwood from Parks Canada assisted with the identification of winter roads and major rivers in snow cover dynamics analysis. Kara Webster and her Canadian Forest Service team provided valuable support and suggestions. We also thank Emily Ogden, Ian Olthof, and Taylor Biccum from the Geomatics Section of Environment and Climate Change Canada for providing us with a land cover map, a peat thickness map, and a sub-pixel water fraction map over the HBL. The Mushkegowuk Council Lands and Resources Department provided opportunities for us to share our work with members of Aboriginal communities and learn from them. Adam Kirkwood and Pascale Roy-Léveillé (Université Laval) provided insightful and helpful discussion around the terrain deformation signals over permafrost landforms. In addition to fieldwork assistance and data sharing, the Four Rivers Environmental Services Group-Matawa Council co-produced an ArcGIS StoryMap with us, entitled “Finding Lichen for Caribou) in three languages (English, French, and Cree) <https://storymaps.arcgis.com/stories/2bb940b2d3bd4d94b5dea08169c12bf3>.